Development of a Three-Dimensional *In Vitro* Tissue Model of the Human Lung Alveolus

A thesis submitted by

Heather Zukas

In partial fulfillment of the requirements for the degree of

Master of Science

In

Bioengineering

Tufts University

August 2017

Advisor: David L. Kaplan, PhD

Abstract

There are currently limited models available for effectively studying lung diseases and drug response aside from animal and clinical trials. This is due to the complexity of the lung's structure and function. The goal of this project was to develop a proof of concept three-dimensional tissue model of a human lung alveolus capable of replicating the ventilation cycle using a silk-based hydrogel. This hydrogel provides a scaffold to incorporate a wider range of lung tissue components, including proteins and cells, as compared to current cell culture models. The material properties of the hydrogel were examined under physiologically accurate conditions for comparison to the native tissue.

With additional modification, this system shows promise of providing researchers with an *in vitro* model that more closely replicates the complexities of the lung as compared to current research options.

Acknowledgements

I sincerely thank Dr. David Kaplan for your guidance and motivation on this project. I would additionally like to thank Dr. Gary Leisk for your input on various ideas and for serving on my thesis committee as well as Dr. Lauren Black III for serving on my thesis committee.

I am also grateful for the help and support from the rest of the Kaplan Lab. You were a very welcoming group and your willingness to answer questions and teach me techniques have been invaluable. Of the group, I am especially grateful to Aswin Sundarakrishnan for teaching me necessary processes and protocols as well as offering suggestions and help when needed.

Lastly, I would like to thank my parents, siblings, and the rest of my family and friends. Your support and encouragement throughout my entire educational career has made this all possible.

Table of Contents

Abbreviations

Abbreviation	Term
COPD	Chronic Obstructive Pulmonary Disease
UV	Ultraviolet
ECM	Extracellular Matrix
DMEM/F12	Dulbecco's Modified Eagle Medium: Nutrient Mixture F-12
HBSS	Hanks’ Balanced Salt Solution
PBS	Phosphate-buffered Saline
FBS	Fetal Bovine Serum
TNS	Trypsin Neutralizing Solution
Pen-Strep	Penicillin Streptomycin
NaOH	Sodium hydroxide
HRP	Horseradish peroxidase
H2O2	Hydrogen peroxide
NDRI	National Disease Research Interchange
PFA	Paraformaldehyde

List of Tables

List of Figures

Chapter 1: Statement of Purpose

The first objective of this project was to provide a proof of concept model of a three-dimensional *in vitro* model of a lung alveolus using a silk-based hydrogel capable of mimicking the human ventilation cycle. The development of this model will allow researchers the ability to study lung diseases within a physiologically relevant *in vitro* cell culture model. Currently, animal models are the leading vector for studying these diseases. Major obstacles lay in the way of animal studies however. Not only are they costly, they can be time consuming and results are not always transferrable to humans. To date, most cell culture tissue model alternatives to these animal models are static, 2D cultures and therefore do not replicate important mechanical properties associated with ventilation. The development of a cell culture tissue model which can incorporate the mechanical stimulus of the lung along with the complex interactions between the cells and ECM could have a wide impact in the medical field, with one of the most important impacts being an equivalent model to animal models to study various lung diseases and conditions as well as test treatments for them.

The second objective of this project was to further define the mechanical characteristics of the hydrogel being used as the tissue model. A silk-based hydrogel previously developed was examined for similarities to the mechanical properties of native human lung tissue. Human lung tissue was analyzed for comparison with this hydrogel.

Chapter 2: Background

The mammalian respiratory system is responsible for circulating air in and out of the body (ventilation) to transfer oxygen into the bloodstream and remove carbon dioxide (respiration). While the respiration process is essential to survival and can be hindered when a disease is present, it was excluded from the scope of this project.

2.1 Lung Anatomy and Physiology

The lungs are the primary organs within the respiratory system. Their responsibility within the body is to transfer oxygen to the blood from the air and collect carbon dioxide from the blood to release to the air. The air travels from/to the mouth and throat, through the trachea. The trachea divides into two bronchi just before reaching the lungs. Once inside the lung tissue, the bronchi divide into smaller branches called bronchioles. At the end of each bronchiole is an alveolar sac containing millions of microscopic thin-walled, spherical air sacs called alveoli (see Fig 1). The alveoli are where the gas exchange with the blood occurs. In total, there on average 480-500 million alveoli in a pair of adult human lungs [38]. Each alveolus within the lung is has an approximate volume of 4.2×10^{-6} mL[38]. The alveoli are wrapped in a vast capillary network which is responsible for delivering oxygen from the alveoli to the body and bringing the waste carbon dioxide from the body to the alveoli.

The lungs are located within the thoracic (chest) cavity protected by the thoracic wall. The thoracic wall is composed of the rib cage along with layers of skin and muscle. Along the inner wall is a thin membrane called the outer (parietal) pleura. A similar pleura, the inner (visceral) pleura, wraps the outside of the lungs. The pleural cavity, the space between the two pleura membranes, contains a thin layer of fluid which acts as a lubricant to allow the lungs to move smoothly within the chest cavity as it expands and contracts.

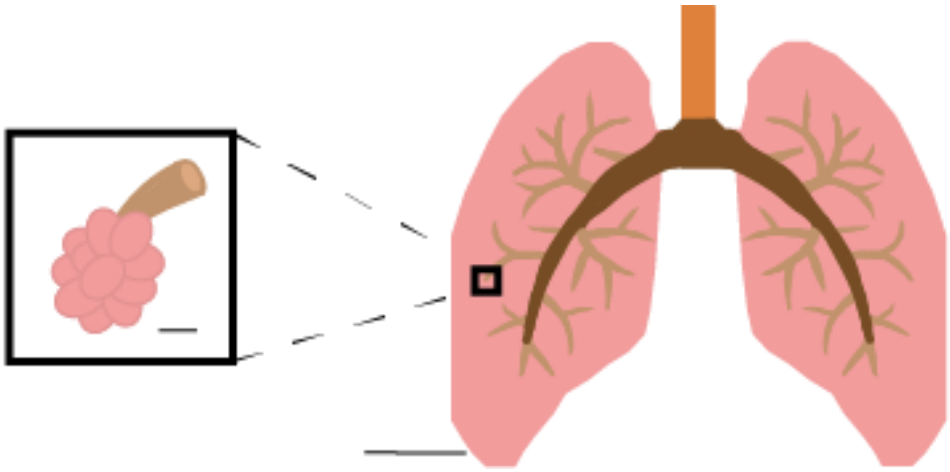

Figure 1: Schematic of the human respiratory system. The trachea (orange) extends down the throat and branches into two bronchi (brown) just before entering the lungs. Inside the lungs, the bronchi branch into millions of bronchioles (tan). A cluster of alveoli (inset- pink) is located at the end of each bronchiole. The inset scale is 200 μm and then outset scale is 50 mm.

2.1.1 Pulmonary Ventilation

Pulmonary ventilation is the cycle commonly referred to as breathing. During this cycle, fresh air rich in oxygen in drawn into the lungs, the oxygen is exchanged for carbon dioxide across the alveolar-capillary wall, and the carbon dioxide rich air is expelled from the body. The pressure-volume relationship described by Boyle's Law is the mechanism that drives pulmonary ventilation. There are three main pressures of interest during the ventilation process: atmospheric pressure, intrapleural pressure,and intra-alveolar (intrapulmonary) pressure. The difference between the intra-alveolar and intrapleural pressures is known as the transpulmonary pressure. In a healthy lung, the transpulmonary pressure is always slightly positive. This positive pressure, is necessary to keep the alveoli open.

This ventilation cycle is composed of two main steps, inspiration (inhalation) and expiration (exhalation). At rest, pulmonary ventilation occurs between 12-20 times a minute. The resulting maximum strain on the lung tissue is approximately 15% during normal ventilation ("quiet breathing") and occurs at the point of maximum diaphragm contraction. The lungs will not fully inflate during "quite breathing". In fact, the tidal volume is, only approximately 10% of the total lung volume. The volume of air inspired will increase during heavy breathing from increased activity such as running.

2.1.1.1 Inspiration

Inspiration is the process of drawing air into the lungs. To begin, the diaphragm and intercostal muscles contract. As these muscles contract, the volume of the thoracic cavity increases. The volume of the plural cavity increases with the thoracic cavity, causing a decrease in intrapleural pressure. This decrease in pressure forces the alveoli to expand, drawing air inward, such that the intrapulmonary pressure is approximately equal to the intrapulmonary pressure. At this point, the intrapulmonary pressure will be below the atmospheric pressure.

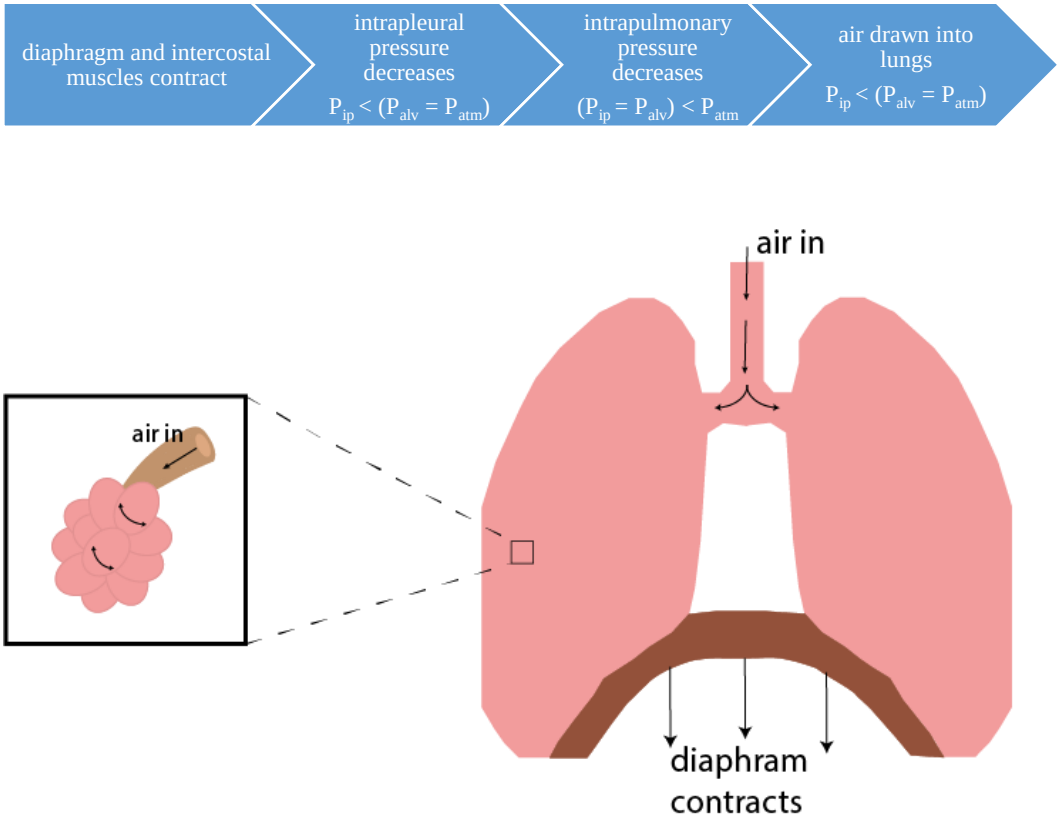

Figure 2: (Top) Flow diagram of the pressure changes responsible for drawing air into the lungs. (Bottom) Diagram of the process as the diagram contracts and air is pulled into the lungs, expanding the alveolus.

2.1.1.2 Expiration

Once the intrapulmonary and intrapleural pressures are balanced, expiration begins. At the inflection point between inspiration and expiration, the intrapulmonary pressure will be lower than the atmospheric pressure. Expiration occurs to increase the intrapulmonary pressure back to approximately atmospheric. As with inspiration, the process begins with the diaphragm and intercostal muscles. These muscles relax, decreasing the thoracic cavity volume. The thoracic cavity volume reduction increases the intrapleural pressure. As this pressure increases, the alveoli are forced to contract and thus force air out to rebalance the intrapleural and intrapulmonary pressure.

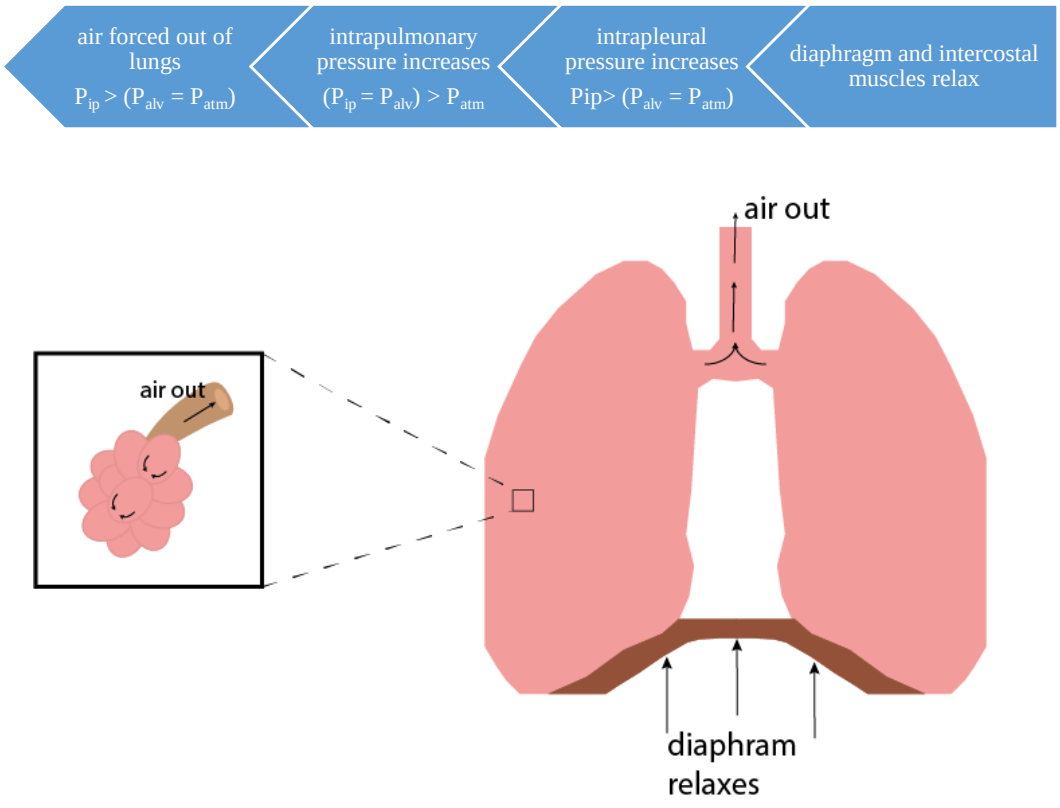

Figure 3: (Top) Flow diagram of the pressure changes responsible for expelling air out of the lungs. (Bottom) Diagram of the process as the diagram relaxes and air is expelled from the lungs, contracting the alveolus.

2.2 Lung Tissue Mechanics

Understanding the mechanics of lung tissue is important for a range of factors including tissue remodeling, cell signaling, and alteration as the result of disease. It has been found that the mechanics driving the ventilation cycle previously described are complex. The tissue alone, neglecting effects of surface tension within the alveoli, exhibit complex, dynamic, nonlinear behavior. This is largely due to how the combination of the fibers, cells, proteins, etc. are arranged within the tissue and how they interact with one another. The alveolar geometries within the tissue are also an important factor that effects the tissue mechanics. The nonlinearity was confirmed in the scope of this project through collection and testing of human lung tissue samples from donor tissue.

The mechanical behavior of the lungs is also effected by surface tension that exists at the air-liquid interface within the alveoli. A thin surfactant film exists inside the alveolus. This film is secreted from the epithelium lining of the alveolar wall and covers the entire inner surface area of the alveolus. The purpose of this film is to lower the surface tension that would otherwise occur at the inner surface of the lung, allowing the alveoli to maintain their optimal shape. Changes in surfactant production has been shown to effect lung performance through a change in the alveolar-capillary shape [46]. The pressure-volume curves of air-filled and liquid filled lungs have been found to have significantly different behavior, signifying the importance of a proper surfactant layer [26, 27].

Effectively incorporating these mechanics into an *in vitro* model will allow researchers to study causes and progression of diseases as well as improve treatment methods without having to use time consuming and costly clinical trials or animal models that cannot be guaranteed to have transferrable results.

2.3 Lung Diseases

Lung diseases effect millions of people worldwide and collectively are currently one of the leading causes of death. Of these, pulmonary fibrosis, pulmonary edema, and COPD are three of the most common. Regardless of the classification of the disease, restrictive or obstructive, there is an abnormality of the lung tissue mechanics that result from the presence of the disease. The mechanical abnormality caused by these diseases impact the patients' ability to breathe, therefore limiting the amount of oxygen brought into the lungs to be circulated through the body. Treatment options do exist for these diseases however most are currently not curative.

2.3.1 Pulmonary Fibrosis

Pulmonary fibrosis occurs when the lung tissue becomes scarred. As with external scars experienced on the skin, the tissue surrounding and between the alveoli will become thicker and stiffer than normal, limiting the ability to expand the alveoli to the necessary dimensions. It is estimated that around 150,000 people

in the United States and 5 million people worldwide currently suffer from this disease, most of whom are over the age of 50.

Pulmonary fibrosis can be caused by long term exposure to occupational or environmental toxins, autoimmune diseases, or as a side effect of certain medications. Despite this, in most cases doctors are not able to determine the reason for onset, known as idiopathic pulmonary fibrosis. In approximately 10-15% of patients diagnosed with idiopathic pulmonary fibrosis have a family member with the disease. Genetic mutations have been linked to the disease however this knowledge is still rudimentary.

While there is no cure to reverse the effects of pulmonary fibrosis, there are treatments available to ease the symptoms. From a medical perspective, one of the largest challenges of pulmonary fibrosis is the wide variation from person to person. For some, symptoms may worsen over a course of months to years while for others they may worsen within a matter of weeks [1].

2.3.2 Pulmonary Edema

Pulmonary edema is a condition that results in excess fluid buildup within the alveoli resulting from fluid leaking from the capillaries. This inhibits the ventilation cycle from working properly as well as prevents proper gas exchange across the alveolar- capillary barrier.

This condition commonly occurs from pressure buildup within the capillaries due to one of many heart conditions. Other factors that can cause

pulmonary edema are trauma, medications, exposure to certain toxins, and prolonged exposure to high-altitude. Supplemental oxygen is generally the first step in treatment of pulmonary edema, regardless of the cause. Depending on the cause, medication is usually given to combat the underlying condition [45].

2.3.3 Chronic Obstructive Pulmonary Disease

COPD generally encompasses two main conditions, emphysema and chronic bronchitis. As the name suggests, COPD is defined as chronic obstruction of the airways. For emphysema, the lining of the alveoli will deteriorate, causing a larger, abnormally shaped alveolus to form from multiple smaller, normal alveoli. Chronic bronchitis is characterized by thickening of the lining of the bronchial tubes, limiting airflow and increasing mucus build up. Collectively, the conditions defined under COPD affect millions of Americans, let alone worldwide. Like pulmonary fibrosis, COPD occurs in higher percentages in populations over 40.

COPD most commonly stems from long time first or second-hand smoke exposure (cigarettes, cigars, etc.). Airborne work and environmental toxin exposures can lead to COPD as well. While there is no cure, there are treatments available to ease symptom's and slow the progress of the disease [62].

2.4 Cell Culture Models for Studying Lung Disease

2.4.1 Static 2D Culture Method

2.4.1.1 Overview

Static 2D cell culture is a traditional cell culture method that examines monolayers of a given cell. This is conducted on either tissue cultured treated plastic or an ECM such as collagen. This method has been used in countless studies in the field, both in academic and industry settings. Because of this, it has become a well-documented, standardized method for studying cell morphology and physiologic response, among other properties. The uniformity and consistency of this method allows for high throughputs, an important factor in industry. This method is also relatively inexpensive, making it an attractive research method in both settings.

2.4.1.2 Limitations

Regardless of the origin within the body, tissue is not composed entirely of a single cell type. The different cell types within the tissue interact with one another as well as the surrounding proteins, etc. within the ECM. In 2D cultures, it is not possible to study these interactions. For cells such as fibroblast which are located within the ECM rather than outside like epithelial cells, 2D static cultures are unable fully model their behavior. With no mechanical stimulation introduced to these cultures, any change in cell behavior due to dynamic motion go unstudied.

2.4.2 Dynamic Culture Model

2.4.2.1 Overview

The leading research in dynamic cell culture models for lung tissue modeling is out of the Wyss Institute at Harvard University [18,47]. Their model, known as a “lung-on-a-chip”, is a microfluidic device that uses etched channels of PDMS to mimic the alveolar-capillary barrier. The device is comprised of three parallel chambers. The two outer chambers are vacuum chambers necessary to create the motion of breathing. Within the middle chamber, there is an additional PDMS membrane running perpendicular to the two outer chambers. Figure 4 shows a cross section of this configuration. One side of this porous PDMS membrane is seeded with alveolar epithelial cells while the other is seeded with microvascular endothelial cells, creating a replication of the alveolar-capillary barrier. This device has had success replicating white blood cell response to bacteria as well as mimicking pulmonary edema. The work done to imitate pulmonary edema has shown the importance of a dynamic model over a static one as pulmonary edema was only experienced when the device was subjected to cyclic vacuum [18].

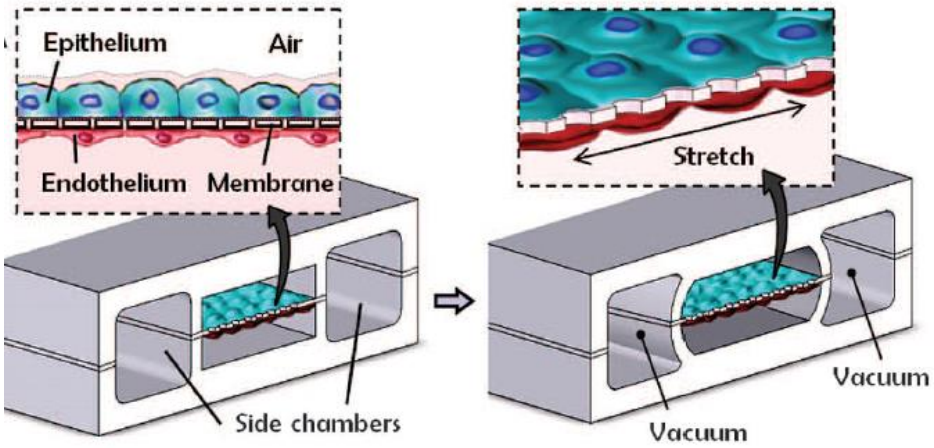

Figure 4: From Huh, D., et al., Cross section of the Lung-on-a-Chip microfluidic device developed by the Wyss Institute. A thin, porous PDMS membrane is seeded with epithelial and endothelial cells to replicate the alveolar-capillary barrier. The two side chambers apply a cyclic vacuum to mimic physiological breathing [18].

2.4.2.2 Limitations

PDMS is widely used for many medical applications due to a range of desirable properties. For this application however, there are some downfalls to using this material. By nature, PDMS is a hydrophobic material and must be treated to reduce the hydrophobicity for cells to adhere and grow. This can be accomplished either through UV or oxygen plasma treatments or by the addition of ECM proteins such as fibronectin or collagen. Because of this, cells cannot be seeded within the PDMS. Using a PDMS membrane to simulate the bulk of the alveolar wall limits the ability to study the interaction between cells and the components of the ECM they are seeded within and the associated mechanical complexities. While this is acceptable for examining the epithelium and endothelium monolayers, to study diseases such as pulmonary fibrosis it is necessary to incorporate fibroblast cells within the model substrate.

The design of the system provides uniaxial tension and compression the PDMS membrane during use. While this is a step above static culture, the lungs undergo biaxial tension and compression which may prove to result in different cell behavior.

Chapter 3: Bioreactor Design Process

3.1 Introduction

There were three critical components to be determined during the design and development process. These were:

1. engineered tissue alveolus
2. self-contained bioreactor chamber
3. mechanism to provide continuous ventilation

Several factors were considered while developing the design for this bioreactor. Since this system involves the use of biological material, sterility was critical for all components that the material would be exposed to. Autoclaving components though the use of high temperature steam was one option for fast sterilization of materials. For components that cannot withstand the high temperature of the autoclave, soaking the parts in 70% ethanol was an effective, convenient alternative, as was UV sterilization. Along with sterility, biocompatibility was another critical component to comply with for materials the alveolus will be exposed to and housed within.

The assembly time and design complexity were also taken into consideration while creating the system design. After assembly of the chamber and lid components, attachment of the alveolus and any future manipulations need to be conducted aseptically within a laminar flow hoods to prevent contamination. From this, all manipulations and assembly steps after this point should be simple

enough to complete using sterile tools. Despite modeling a complex human organ, the system should be simple enough to construct such that it is replicable with minimal to no variation.

3.2 Alveolus

Using SolidWorks CAD software, renderings were created for the mold which the engineered alveolus was cast in. The molds were designed in a spherical shape with a cylindrical offshoot. This shape was chosen as native alveoli are most similar to hollow spheres and are modeled as such in a majority of computational models. The cylindrical offshoot mimics the bronchiole that the native alveoli are attached to. Two types of molds were created; one for the engineered alveolus construct to be directly cast in and one which would be used to create a PDMS mold which the alveolus would ultimately be cast in. Both models are shown in Figure 4. The CAD files were transferred to a 3D printer to be printed using ABS plastic. The alveolus scale chosen was 20mm in diameter. Both PDMS and ABS plastic can be sterilized through methods previously discussed. For both mold types, two identical halves were printed to be secured together before creating the engineered alveolus and separated to remove the alveolus after gelation.

The purpose for creating two casting methods was to compare the nonstick capabilities of the two materials with the hydrogel. The hydrogel must release

from the chosen mold with relative ease to ensure that no holes or rips were introduced while transferring the construct from the mold to the chamber.

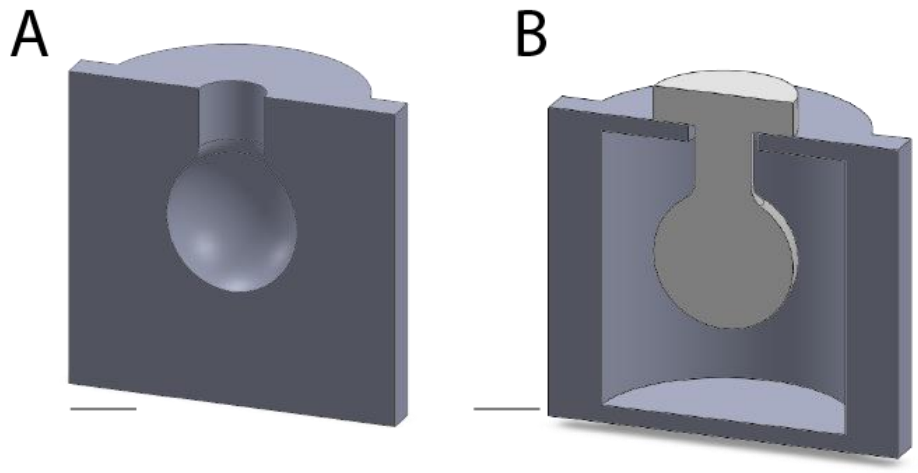

Figure 5: Isometric drawings of (A) design one, to cast the hydrogel directly in the 3D printed mold and (B) to use the 3D printed mold to cast a PDMS mold to ultimately be used to fabricate the hydrogel model. Scales shown are 10mm.

It was determined that there was no significantly noticeable difference in the ease of hydrogel release between the two mold materials. With this conclusion, the plastic molds were generally used for the sake of simplifying the construction process.

Along with two different models for the mold itself, two different approaches for the design of the engineered alveolus were taken. The first approach was designed such that the gel model would consist of a spherical alveolus with a bronchiole segment extending from the top. At the top of the bronchiole would be a washer-like anchor designed to suspend the alveolus construct within the system. All components of this model were composed of the silk-collagen hydrogel (see Figure 6). The advantage to this method was that it

was not necessary to attach the construct to another material in order to suspend it within the chamber. However, this required a more complex lid design to seal the system, as will be discussed in 3.3, and to suspend the alveolus. Additionally, this method required ensuring that the hydrogel section anchoring the alveolus to the top of the chamber would have the structural integrity necessary to hold the weight of the rest of the alveolus construct while suspended.

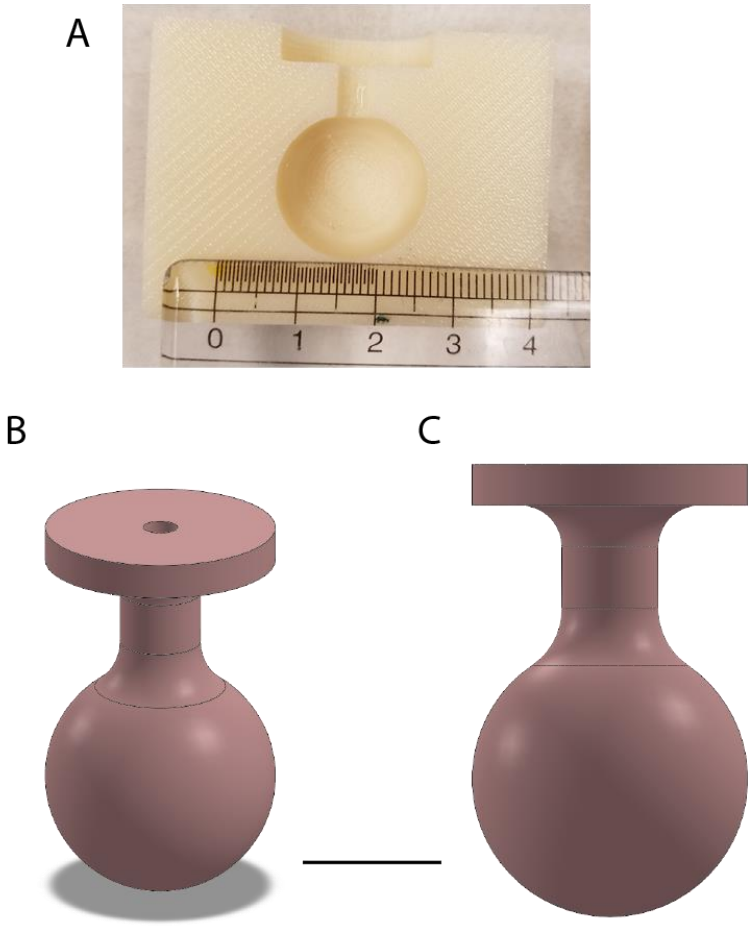

Figure 6: (A) 3D printed mold which was used to cast the all hydrogel alveolus. Ruler units shown in cm. (B) Isometric and (C)head on drawings of the engineered alveolus fabricated from only hydrogel. Sale shown is 10mm.

The second approach was to eliminate the hydrogel anchor portion of the first approach and suspend the alveolus within the chamber by securing the bronchiole section to a segment of flexible tubing. The segment of tubing would extend through the chamber lid, eliminating the need for the hydrogel anchor. Eliminating the hydrogel anchor simplifies the chamber lid, as will be discussed in 3.3. This design also places some of the stress of suspending the alveolus onto the tubing. However, since this design relies on connecting two materials, a clamp was needed to fasten them together. This placed a targeted stress on the hydrogel at the edges of the clamp. The clamp needed to be able to fasten the hydrogel tight enough to the tubing that it would create an airtight seal between the two without hindering the airflow within the tubing or breaking the hydrogel.

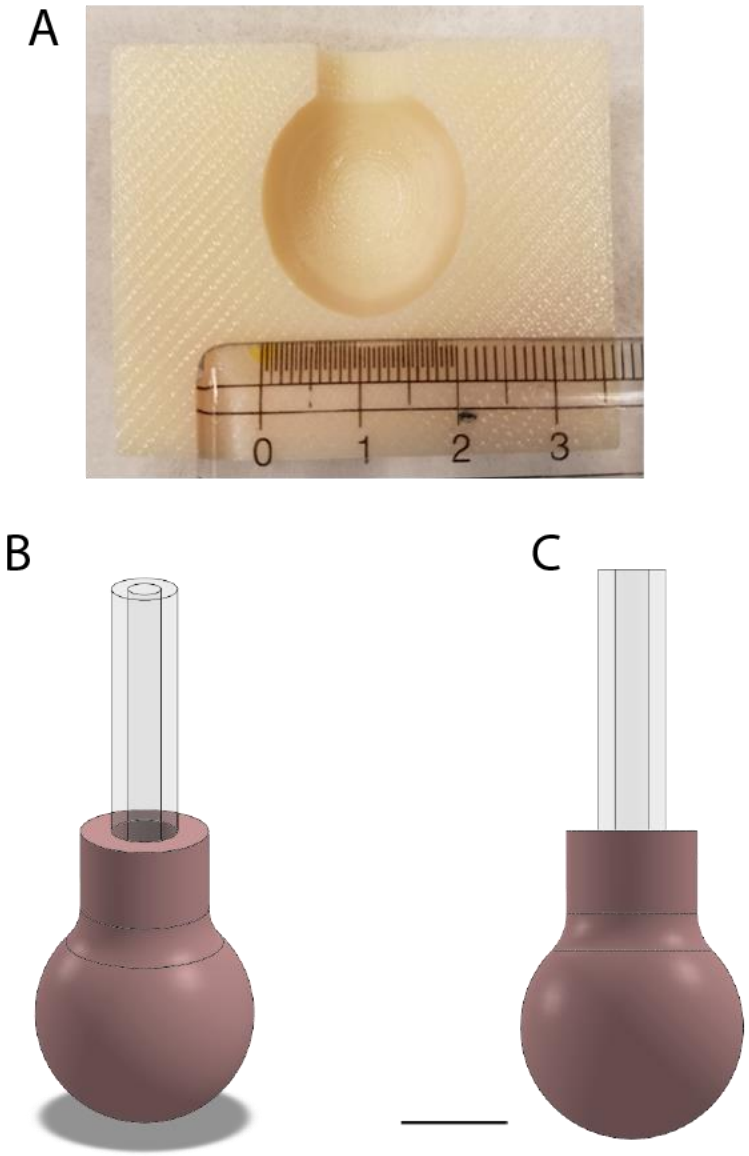

Figure 7: (A) 3D printed mold which was used to cast the alveolus which was connected to a tubing segment. The ruler shown gives units in cm. (B) Isometric and (C)head on drawings of the engineered alveolus and bronchial construct (pink) with a section of tubing inserted. The filter attached
to the top of the tubing and the clamp fastening the construct to the tubing are not shown. Sale shown is 10mm.

Beyond casting the engineered alveolus within a mold, a method for creating a cavity within the alveolus had to be developed. This was necessary to create a balloon like model. To be successful, the chosen method needed produce a uniform wall thickness throughout the hydrogel, could be suspended within the hydrogel during gelation, and be easily removed without damaging the hydrogel once fully set. Additionally, as with the rest of the construction materials, the method for creating the cavity had to be sterile.

One method investigated was the use of an inflatable device, such as a balloon, to create the cavity. The device was inflated to the desired diameter and suspended within the hydrogel mold before securing the hydrogel mold together for inserting the hydrogel solution. The hydrogel solution was then injected into the mold and placed in an incubator to set. Once fully set, the inflatable was deflated and carefully removed from the cavity. The cavity was then rinsed with PBS and filled with cell culture media. With this method, it could be difficult to ensure uniform diameter of the inflated sphere across multiple samples. The advantage of this method is that it does not need to sit at room temperature for an extended period, like the other method to be discussed. Since it can be placed directly in the incubator after injecting the hydrogel into the mold, there is little concern for cell death during the gelation process through unfavorable conditions.

Another method investigated was a method commonly used for creating microchannels within microfluidic devices known as the sacrificial gelation method. For use in microchannel fabrication, a gelatin mesh is first created within a negative PDMS mold. The mesh is then transferred to the hydrogel mold,

surrounded by the hydrogel solution, and left to cure at room temperature. Once fully gelled, the sacrificial gelatin is liquified by placing the construct in 37°C. Once back to a liquid state, the gelatin solution can be flushed from the construct using PBS, leaving the channel shape fully intact.

A similar approach could be used for the development of the hollow alveolus. A gelatin mold of identical shape but smaller diameter would be crafted and placed inside the larger mold. The larger mold would then be filled with the hydrogel solution and left to set before placing in 37°C to liquify the gelatin. The liquid gelatin would be removed with a manual pipette and the cavity would then be flushed with PBS to remove any remaining gelatin before filling the cavity with cell culture media. This method would provide uniform alveolus walls across multiple samples however assembly time would be increased through the need to set the gelatin along with having to set the hydrogel at a lower temperature. The longer set time at room temperature may prove to be unfavorable to fibroblasts once introduced into the system.

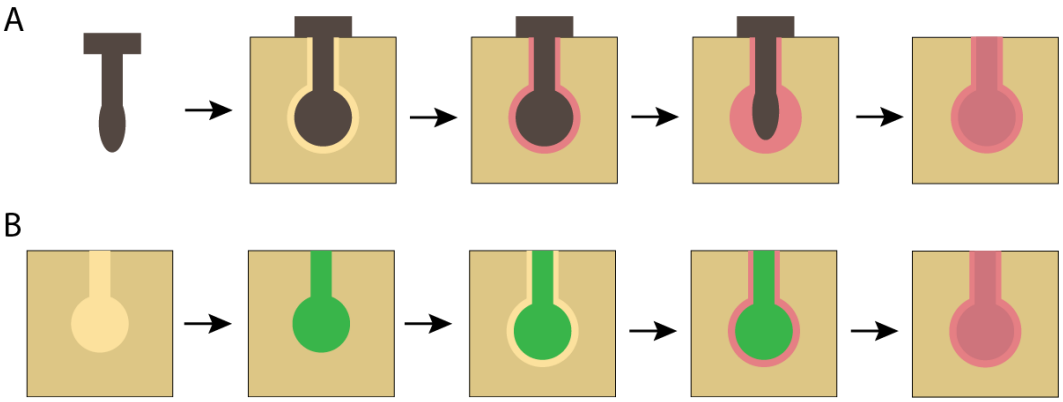

Figure 8: (A) Cross sectional view of the process of creating the alveolus model using the inflating insert method. An inflatable insert is placed within the hydrogel mold. The hydrogel (pink) is injected into the mold and left to set. Once the hydrogel is fully set, the inflatable in deflated and removed, leaving a negative cavity within the inside of the hydrogel. (B) Cross sectional view of the process of creating the alveolus model using the sacrificial gelatin method. A negative mold is filled with gelatin (green) and felt to set. The gel is then transferred to a larger mold. The hydrogel (pink) is injected into the larger mold and left to set. Once the hydrogel is fully set, the mold is placed in an incubator to liquify the gelatin, leaving a negative cavity within the inside of the hydrogel.

3.3 Chamber and Lid

The system, like the human lung, relies on a pressure differential to draw air in and out of the engineered alveolus. Because of this, the entire chamber must be completely air tight. Even the smallest hole could allow air into the system and limit the effectiveness of the system's performance.

3.3.1 Chamber

The initial design concept for the chamber included a solid sided cylinder with a flexible, silicone membrane separating two chambers. This membrane would contract and relax to increase or decrease, respectively, the volume of the chamber. To create the vacuum under the silicone membrane necessary to stretch the membrane, a custom designed chamber would be created. In this, the membrane would sit between two chambers. The upper chamber would contain the alveolus and media while the lower chamber would contain only air (Fig. 9). The change in volume as the membrane contracts and relaxes through vacuum would create a pressure differential like that experienced within the lung and thoracic cavity when the diaphragm contracts and relaxes.

The second design for the container was constructed through modification of a small, cylindrical jar. Two holes would be drilled across from one another into the bottom of the container as inlets. The inlets allow media to flow in and out of the chamber at a determined rate. Rubber grommets added within the inlets

eliminate any rough edges that may be present after drilling and further insure an airtight seal. The rubber tubing used for media flow would be inserted directly through the grommet (shown in red in Figure 9) into the bottom of the container. The withdrawal of media creates a negative pressure differential between the syringes and the inside of the alveolus, forcing air from the atmosphere into the cavity to regulate the pressure change. Conversely, when the syringes pump media back into the chamber, the pressure within the syringe and chamber will increase, forcing air out of the alveolus, again to regulate the pressure change.

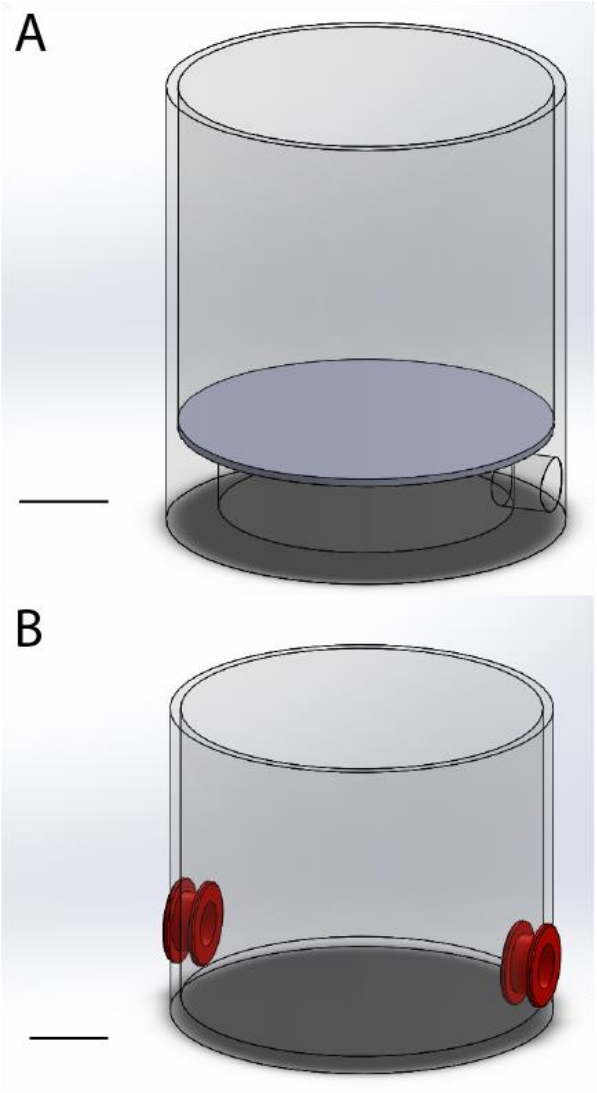

Figure 9: Isometric drawings of the two designs for the chamber which would house the alveolus model. (A) A custom-made chamber would be cast out of a material such as Delran and a thin silicone membrane (shown gray) would be attached to the inside to separate the two chambers. (B) A premade plastic jar would be modified with the addition of two hole to accommodate blunt end needles. Scale shown in 20mm

3.3.2 Alveolus Suspension and Chamber Cover

Three concepts were developed to hold and suspend the engineered alveolus while sealing the system and prevent contaminants from entering. These concepts were tailored to the two alveolus designs. One was designed for the combination hydrogel and tubing design and two for the fully hydrogel design.

Hydrogel and Tubing Design

For this design, a single hole was drilled through the center of the lid and a grommet was placed inside. The segment of flexible tubing used to suspend the hydrogel alveolus was then inserted through the grommet. To prevent potential contamination as air passes through the tubing into the alveolus, a filter was attached to the end of the tubing that was exposed to the surroundings. Since the hydrogel is not exposed to any part outside of the chamber or lid, no secondary cover is necessary beyond the filter to limit environmental exposure.

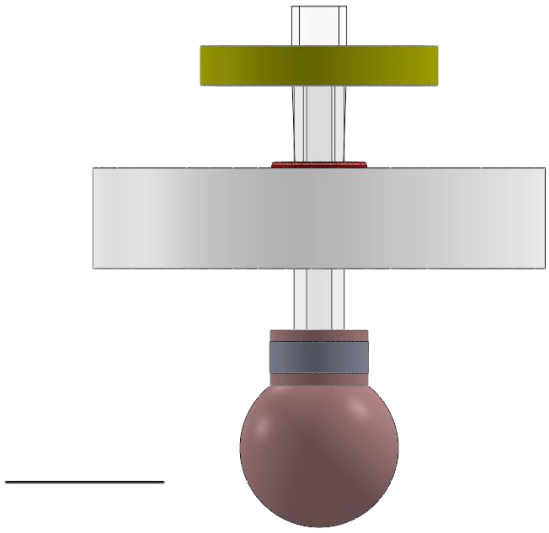

Figure 10: Front view drawing of the alveolus suspension and lid design assembly. The alveolus model (pink) is secured to a segment of tubing through a tube clamp (grey). The tubing extends through the lid and the air that passes through is filtered using a 0.22µm filter (yellow).

Full Hydrogel Design

Two designs were developed to suspend the alveolus and seal the system from contamination for this. Since there is a washer shaped hydrogel segment anchoring the alveolus for suspension, careful consideration had to be taken to ensure this portion would properly suspend the engineered alveolus while providing the necessary airtight function for the system.

The first was to drill a hole through the center of the original lid of the jar just as in the first design discussed. The hole would need to be drilled large enough to carefully manipulate the anchoring segment though but small enough that the anchor is still capable of supporting the hydrogel. Since the hydrogel

anchor sits on top of the original lid, a secondary cover is needed to protect the biological material from external exposure. Casting a simple PDMS cover to fit over the existing lid would fulfill this requirement. Alternatively, a custom cover made of a more robust material such as Delrin would be acceptable.

There were a couple main challenges surrounding this design. The anchor portion of the model would not be covered in media once suspended. Over time, this region of the hydrogel would dry out. Since hydrogels by nature are composed significantly of liquid, the gel would shrink as it dries out. Second, once in place the gap created from the difference in size between the bronchiole and the hole it passes through must be properly sealed to create an air tight inner chamber.

A holder to suspend the alveolus within the chamber would alleviate the challenge of exposing the anchor portion to air for an extended period of time. This design would be made in two halves that would be placed around the bronchiole for the anchor to rest on. The alveolus would be suspended from this holder and would sit completely submerged within the media. Before submerging the alveolus within the media, a segment of tubing would be inserted into the bronchiole of the alveolus model. When the chamber is closed, the tubing segment extends through the lid, as in Figure 11, allowing air flow in and out of the cavity and prevent the alveolus cavity from being filled with media during submersion.

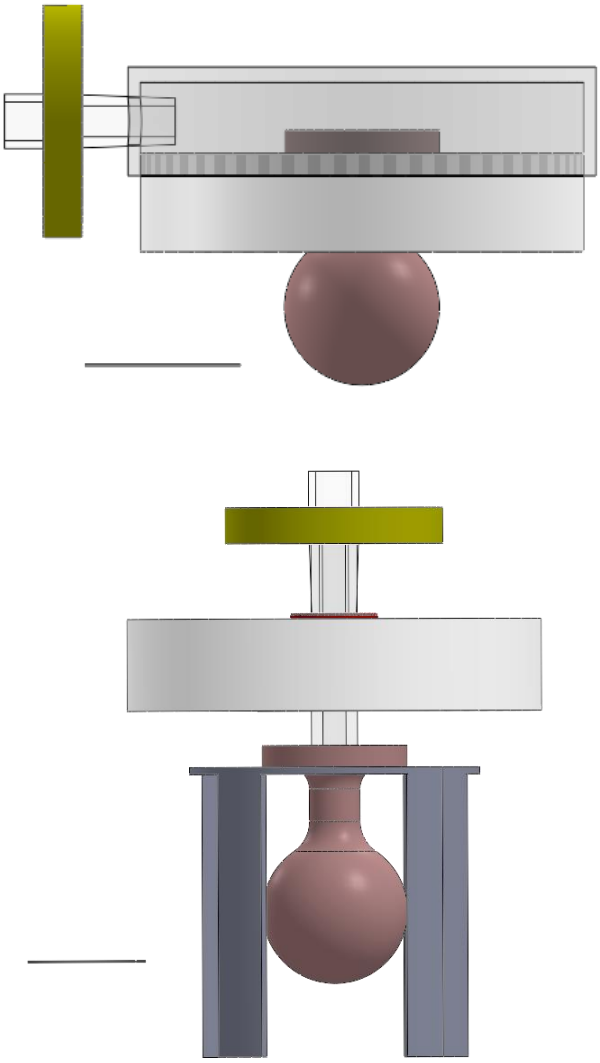

Figure 11: (Top) Face view drawing of the all hydrogel alveolus model (pink) suspended from the original lid of the chamber. A secondary cover protects the hydrogel from contamination, extended by the addition of a 0.22µm filter. (Bottom) Face view drawing of the all hydrogel alveolus model (pink) suspended on a custom-made holder. The holder is in two halves so it can be put into place around either side of the bronchiole segment without manipulation of the hydrogel.

3.4 Mechanism for Simulated Ventilation

Based on the chamber designs created, it was necessary to find a piece of equipment capable of controlled media or air flow. This tool must be easy to program and fine tine based on model parameters. The New Era Pump Systems, Inc. Multichannel Programmable Syringe Pump fit this need. The pump can hold multiple syringes which, in this case, would contain cell culture media or air. The system can be programmed either directly on the device or through a computer program.

3.5 Chosen System Design

After weighing the benefits and limitations to the designs for each component of the system as well as some initial testing, an overall design was chosen. The chosen system limits assembly time and complexity of the chamber as well as limits the amount of handling the hydrogel is introduced to. This system is composed of the following components:

1. Alveolus model that is attached to a segment of tubing
    a. Inflatable mold to create the cavity
2. Chamber that utilizes media flow in and out of drilled inlets
3. The Syringe Pump system to create the cyclic pressure change

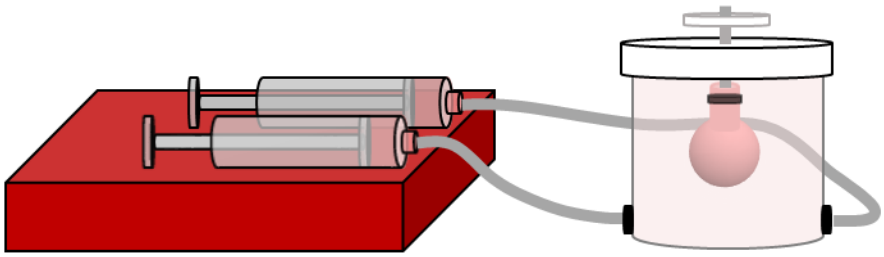

Figure 12: Illustration of the complete system. The syringe pump (left) is connected to the closed chamber containing the hydrogel alveolus model (right). The alveolus is suspended within the chamber though connection to a segment of flexible tubing. The air is filtered before entering the system through a sterile filter. Note: Not drawn to scale

Before creating the alveolus from hydrogel to place within the system, a PDMS model was created using the method previously described, modifying the set time and temperature to match the parameters necessary for setting PDMS. With the exception for creating the model under non-sterile conditions, the production method was tested as if the more fragile hydrogel was being created.

To ensure an airtight assembly resulted from the developed method, a substitute alveolus was first tested. For this, a simple balloon was connected to the system as if it were the hydrogel alveolus. Balloons behave similarly to the alveoli within the lung, and are often used as a real-world comparison. Again, the primary function of the balloon model was to ensure the chamber manufacturing process resulted in an airtight system. This also allowed for testing of the pump system to confirm it would meet the needs of the system.

After confirming that the manufacturing process for both the chamber and alveolus were acceptable and that the pump could be programmed to the necessary cyclic flow rate, attempts were made to construct the final product.

Figure 13: System assembly using a PDMS alveolus model in place of a hydrogel model. The media has been withheld for the image. Scale shown in 10mm

Chapter 4: Materials and Methods

4.1 Materials List

4.1.1 Cell Culture Materials

Gibco: DMEM/F12 (#11320033)

Fisher Scientific: Fetal Bovine Serum (MT35011CV)

ThermoFisher Scientific: Trypsin (25300-062), Pen-Strep (1514122)

Lonza: TNS (CC-5002)

Native Tissue: fibroblast cells

4.1.2 Silk- Collagen Hydrogel Materials

ThermoFisher Scientific: Rat tail collagen, type I (CB354249), DMEM (11966025)

Sigma-Aldrich: HRP (P8375-25KU), H_2O_2 (H1009), NaOH (72068)

Flexcell International: Tissue Train Culture Plate- Collagen IV coated (TT-4001C(IV))

4.1.3 Bioreactor Materials

McMaster-Carr Supply Company: Clear Polystyrene Plastic Jar (4188T41), Stainless Steel Dispensing Needles with Luer Lock Connection, 14 Gauge (75165A117), High Temperature Grommets (1061T11), High-Temperature/High-Purity Silicone Rubber Tubing (51845K55), Plastic Quick-Turn Tube Plugs (51525K123, 51525K213)

New Era Pump Systems: Six Channel Programmable Syringe Pump (NE-1600)

Fisher Scientific: Krayden Sylguard 184- PDMS (#NC9285739), HSW Soft-Ject Disposable Syringe (14-817-56), 0.22μm sterile filter (SLGV004SL)

4.2 Hydrogel Fabrication

Hydrogels are hydrophilic, three-dimensional, cross-linked polymer networks. This network results in a soft, elastomeric biomaterial capable of supporting cell adherence and proliferation. Since the biomaterial is hydrophilic after gelation, it can be submersed in cell culture media, or other solution, without dissolving. This is an important characteristic as it is critical for any cell culture platform to allow for the addition of an adequate nutrient source for the seeded cells. Additionally, the degree of cross-linking provides a method for tuning the material to provide structural and functional similarity to various soft tissues, making it an important player in the field of tissue engineering. Silk fibroin, a non-immunogenic, natural polymer, has been studied extensively for use in tissue engineering and hydrogel formation.

4.2.1 Preparation of Silk Fibroin Aqueous Solution

The protocol used was adapted from previously published protocol [29]. Silk fibroin was extracted by cutting *Bobmyx mori* cocoons into pieces then boiled for 1 hour in a sodium bicarbonate solution (4.24g sodium bicarbonate in 2 liters of purified water) to remove the sericin coating. Each 5g batch of silk cocoons were boiled within the 2L sodium bicarbonate solution. After boiling, the silk was rinsed three times with purified water to remove excess solution and left to air-dry. Once dry, the silk fibroin was solubilized in a 9.3M LiBr solution at 60°C for approximately 4 hours. The silk/LiBr solution was then placed within regenerated cellulose tubing (3.5 kDa MWCO) and suspended within in 2L of moving purified water for 48 hours to remove the LiBr from the silk fibroin solution. During this time, the water was changed a total of 6 times. After 48 hours, the solution was removed from the tubing. If necessary, the solution was further concentrated at this point. Before use, the solution was filtered through a Nalgene vacuum filter to remove any impurities. The final silk concentration of the solution was between 9-12% (w/v).

4.2.2 Silk-Collagen Hydrogel Fabrication

Rat tail type I collagen – silk protein hydrogels were fabricated in various sized batches by mixing appropriate amounts of collagen, silk solution, NaOH, DMEM, and ultra-pure water per previously determined protocol. To initiate gelation, H_2O_2 and HRP were added to the solution. Gelation occurs though tyrosine crosslinks of the silk fibroin and collagen. The solution was mixed well

using an electric pipette then plated by pipetting a set volume onto the plate of interest. It was then left to fully set (approximately 30 min) in a 37°C incubator. Once gelation occurred, DMEM/F12 media was added to the plates to keep the gels hydrated as well as provide necessary nutrients to fibroblast cells (see 4.3.1).

4.3 Cell Culture

Human lung fibroblast cells were seeded and maintained in T175 cell culture treated flasks. The cells were maintained with DMEM/F12 cell culture media supplemented with 10% FBS and 1x Pen/Strep. Media was changed once every two to three days. Once cells reached 80-90% confluency, the cells were passaged or used for experimentation.

4.3.1 3D Cell Seeding and Culture

To seed fibroblasts within the hydrogel construct, the following method was used. The cells were dissociated from the cell culture flask using trypsin and then neutralized with TNS. The neutralization of trypsin is critical to prevent it from damaging the cell surface after dissociation. The media and cell solution was collected and centrifuged for 5 minutes to separate the cells from the rest of the solution. After centrifugation, the supernatant was removed and the cells were gently resuspended within fresh media. During this, the cells were concentrated to $20x10^6$ cells/mL of media and added to the silk-collagen hydrogel (as described in 4.2.2) at a concentration of $1x10^6$ cells/mL of hydrogel solution. After gentle

pipetting to ensure even distribution of cells within the solution, the hydrogel was plated into the trough of Tissue Train Culture Plate wells created with the Flexcell Tissue Train System.

4.4 Native Lung Tissue Samples

Human lung tissue specimens were procured through NDRI. Protocol was developed stating smoking history, health history, etc. to ensure the specimens received were healthy and to limit variables that could affect both the mechanics of the tissue and the health of the cells collected from the tissue.

The specimen was sectioned into lobes after procurement. Before further slicing, the section being used was rinsed in a petri dish using HBSS to remove any remaining blood from within the tissue. The lobe was then transferred to a new petri dish to begin dissection. A thin layer of HBSS was added to the dish to keep the tissue hydrated during the dissection process. Using a combination of scissors and a scalpel, the lobe was further sectioned then cut into strips of the desired dimensions. During dissection, regions of the lobe with visible bronchial or bronchiole were avoided. The finished strips were submerged in a sealable container with HBSS until all samples were collected. The samples were then transported on ice to the testing location. A total of four different lung specimens were tested.

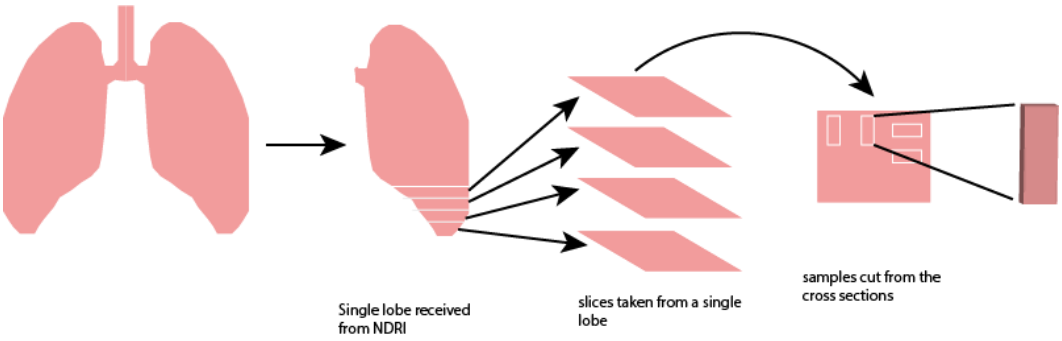

Figure 14: Schematic of the preparation of the native lung tissue samples. Cross sections from a given lung were all cut from the same lobe. Samples were randomly cut from the cross sections. The final dimensions of each sample are 3x5x25mm

4.5 Bioreactor Assembly and Function

As discussed, there are three main components to this system, an engineered alveolus, a chamber to house the alveolus, and a mechanism to induce the ventilation cycle. The bioreactor works on the same concept of cyclic pressure change as the lungs. To achieve this, media was withdrawn from/ pumped into the fully sealed chamber. The pressure drop caused by the media being withdrawn forces air into the alveolus model, resulting in expansion. Conversely, the addition of media back into the camber increases the internal pressure, forcing the alveolus to contract and push air out of the inner cavity.

4.5.1 Assembly

The chamber was constructed using the method described in 3.3.2. After all holes were drilled, the chamber and lid were rinsed with purified water to remove any plastic filings created during the process that remained on the surfaces. After inserting the grommets, these components were sterilized along

with the remaining assembly components. The sterilization process is summarized in Table 1 for all components of the system.

Table 1: Summary of the necessary components to assemble the bioreactor system and the sterilization method for each component

Part	Number per Chamber	Sterilization Method
Chamber		
Lid assembly (with grommet)	1	Ethanol/UV
Reservoir (with grommets)	1	Ethanol/UV
Clipped blunt end needle	2	Ethanol
Filter – 0.2 μm	1	Pre- sterilized
Alveolus Assembly		
3D printed mold half	2	Ethanol/UV
Balloon	1	Ethanol
Tubing	1	Ethanol
Clips	2	Ethanol/UV
Pump Connection		
Syringe – 30mL	2	Pre-sterilized
Quick Turn Plugs – female	2	Ethanol
Quick Turn Plugs – male	2	Ethanol
Tubing	2	Ethanol

After sterilization, the alveolus tissue model was engineered using the silk-collagen hydrogel described in 4.2.2. The hydrogel solution was injected into the mold and left to set within an incubator using the method described in 3.3.1. Once fully gelled, the inflatable mold was removed and media was added to the cavity to ensure that the hydrogel did not dry out. The addition of media will also be important once cells are introduced into the system. The engineered alveolus was left to further set for a day before removing from the mold. Once set, the media was removed from the inside of the alveolus, the segment of tubing used to suspend the alveolus was inserted, and the alveolus itself was removed from the mold. Before placing inside the chamber, the alveolus was secured to the tubing through either a sterilized tube clamp or a zip tie. The alveolus was then moved into the media filled chamber.

4.5.3 Function

Like the human lung, this system relies on the relationship between pressure and volume described by Boyle's Law:

$$P_1V_1 = P_2V_2 \ (eq.1)$$

This relationship states that the product of the pressure and volume of a system must remain constant between any two time points assuming temperature remains constant. Within the engineered system, this relationship is exploited through the removal/ addition of media from the chamber by the expansion/compaction of the

syringe volume. To be comparative to the human ventilation cycle, the engineered system must remove/add the defined volume of media from the chamber at a rate such that the alveolus expands/contracts at a rate that mimics that of a native human lung.

The defined volume of media to be infused/withdrawn was determined from the initial parameters of the engineered alveolus and the maximum strain placed on the lung tissue during the respiration cycle. The volume change of the alveolus was assumed to occur within a spherical, thick walled pressure vessel, neglecting any volume changes that may occur within the bronchiole region. The assumption of a spherical body was made since there is a segment of tubing within the entire bronchiole segment with a higher stiffness than the hydrogel. A pressure vessel is considered thick-walled if the outer radius is 10 times greater than the wall thickness. In the case of the current model, the radius is only 2.33 times greater than the wall thickness. The material is also assumed to be isotropic and incompressible.

The volume change was calculated based on the hoop (circumferential) strain. First, the change in circumference (ΔC) was calculated.

$$\varepsilon = \frac{\Delta C}{C_{o,1}} \rightarrow C_{o,1}\varepsilon = \Delta C \ (eq.2)$$

Where $C_{o,1}$ is the initial outer circumference and $C_{o,2}$ is the maximum outer circumference. This leads to the final radius ($r_{o,2}$)

$$\Delta C = C_{o,2} - C_{o,1} = 2\pi\left(r_{o,2} - r_{o,1}\right) (eq3)$$

Knowing that the overall volume of the hydrogel remains constant, the final inner radius can be calculated.

$$V_W = \frac{4\pi}{3}\left(r_{i,2}^3 - r_{i,1}^3\right) = \frac{4\pi}{3}\left(r_{o,2}^3 - r_{o,1}^3\right) \rightarrow$$

$$r_{i,2} = \sqrt[3]{r_{o,2}^3 - r_{o,1}^3 + r_{i,1}^3} \quad (eq\ 4)$$

The final volume of alveolus as a whole and of just the inner cavity at maximum strain was calculated based on the initial volume and volume change during inspiration.

$$V_f = V_i + \Delta V \quad (eq.5)$$

$$V_f = \frac{4\pi}{3}[(r_i + \Delta r)^3 - r_i^3] \quad (eq.6)$$

The change in volume of the alveolus as a whole was used to calculate the volume of media to remove. As media is withdrawn/infused into the chamber, the overall volume of the chamber and syringes change, resulting in the desired pressure differential. This volume was converted into a flow rate based on the number of respiration cycles the average adult completes per minute. The Syringe Pump was then programed to infuse/withdraw the desired volume at the necessary rate.

$$\frac{\#\ respiration\ cycles}{min} * \frac{\#\ steps\ (inspiration + expiration)}{cycle} * \frac{\mu L}{step}$$

$$= \frac{\mu L}{min}\ (eq. 7)$$

Two 60mL syringes were loaded into the pump system, each connected to one of the tubing sections designed to add or remove media from the chamber. Since two syringes were used for a single chamber, the flow rate calculated was divided in half before programming it into the pump.

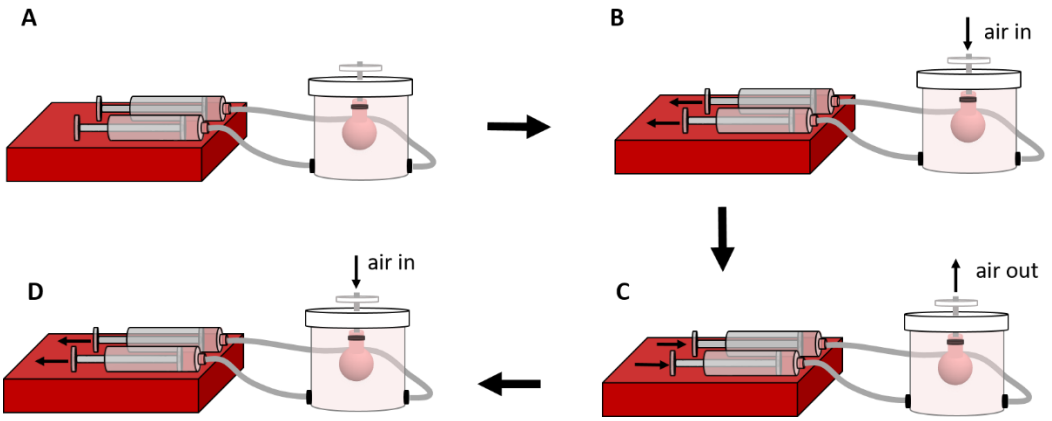

Figure 15: Illustration depicting the inspiration and expiration of the engineered system. (A) The system is shown at rest, with the engineered alveolus at its initial volume. (B) As the syringes are withdrawn, air is forced be drawn through the filter into the engineered alveolus to balance the pressure decrease from the loss of media within the reservoir. This results in an increase in the alveolus volume. (C) The syringes are depressed, injecting media into the reservoir, forcing air out of the alveolus to balance the increase in pressure. This decreases the alveolus volume back to the initial volume. (D) The process is repeated

4.6 Data Acquisition

4.6.1 Instron

Analysis on native tissue samples was performed using the Instron 3366 Uniaxial Tensile Testing Systems. This was done to determine the elastic modulus. Sandpaper was added to the inside of the grips of the instrument to reduce the chance of the sample slipping during testing.

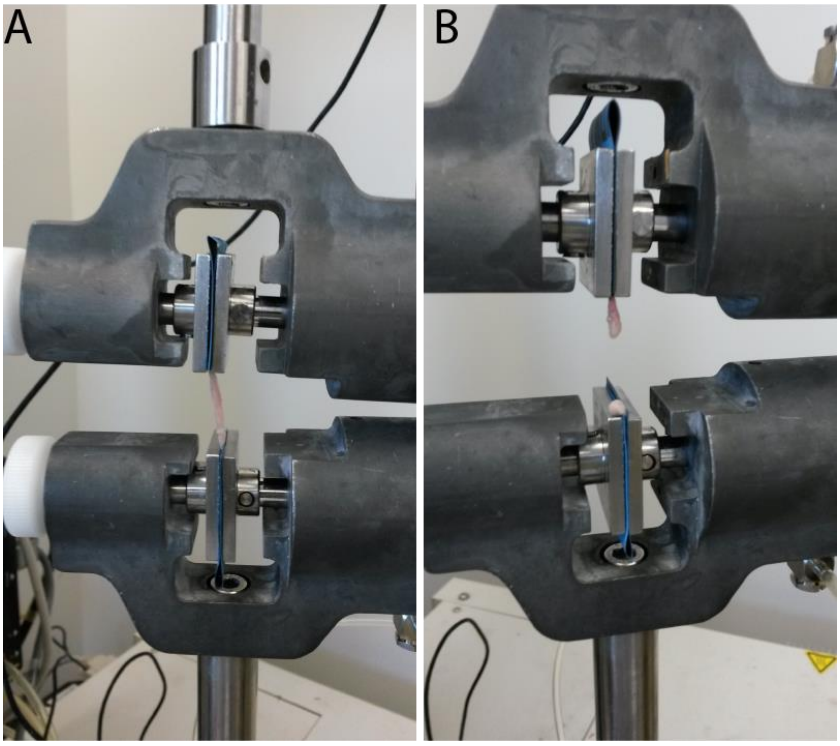

Figure 16: Native lung tissue Sample (A) before beginning the test and (B) after failure occurred. The blue slivers at the top and sides of the grips are the edges of the sandpaper placed between the grips to help hold the tissue samples are

4.6.2 DMA

The TA Instruments RSAIII Dynamic Mechanical Analyzer was used to examine hydrogel mechanical properties after cyclic loading. To ensure the samples did not dry out during this analysis, all tests were conducted within a bath of saline (PBS). The instrument was prepped by connecting the necessary grips and zeroing the load cell. Samples were loaded into the instrument one at a time with the addition of sandpaper between the grips to further ensure that the sample did not slip during testing Samples were testing under two loading conditions, one mimicking the average ventilation cycle and one using parameters from the single load test. After the desired number of cycles, the samples were loaded until failure. The data collected from the final load was used to determine the tangent modulus.

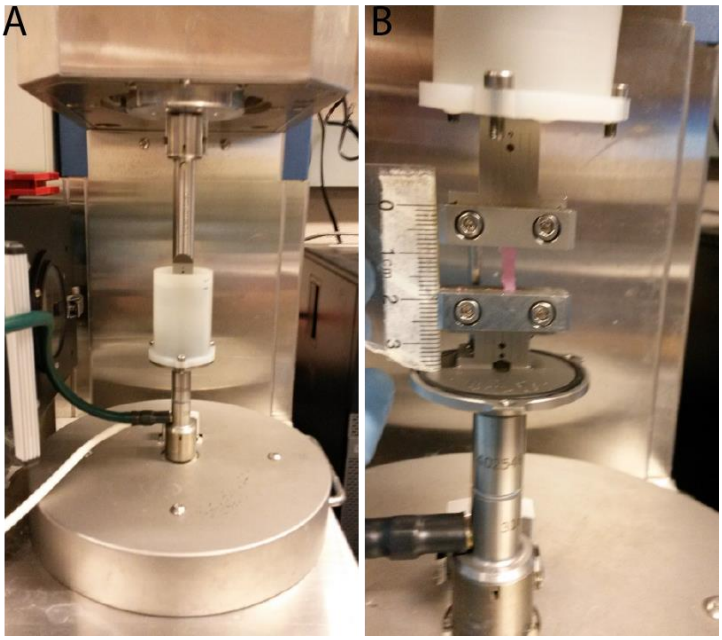

Figure 17: (A) Setup for cyclic loading of a hydrogel samples within a PBS bath. (B) The hydrogel samples just after loading before securing and filling the bath casing for testing. The ruler shown provides units in cm.

4.6.3 Histology

Native tissue samples were fixed with 4% PFA after collection. The samples were then placed in an automatic tissue processor which dehydrated, cleared, and embedded the samples with paraffin. Once finished, the samples were embedded within a paraffin block. The paraffin blocks were sectioned at 5μm using a microtome and the sections were placed on slides to be stained. H&E staining was performed to identify the tissue morphology and cell morphology as well as cell location. After staining, cover slips were secured over the samples on the slides.

Engineered tissue samples were fixed with 4% PFA after collection and then manually dehydrated through a series of graded ethanol. As with the native

tissue, the samples were paraffin embedded and sectioned at 5μm after dehydration. These samples were stained with H&E as well as Alcian Blue.

All slides were imaged using a Keyence fluorescence microscope. Images were captured using brightfield. A series of different magnifications were used to capture multiple locations within each sample.

4.6.4 Statistical Analysis

All statistical analysis was conducted using GraphPad Prism (GraphPad Software, Inc.). Outliers within the native tissue dataset were determined using ROUT analysis before calculating the mean and standard deviation for comparison to the hydrogel. Unpaired t-tests were performed to determine statistical significance between the means of two groups. When comparing multiple groups, one-factor ANOVA analysis was performed to determine statistically significant variance along with Tukey's multiple comparison test.

Chapter 5: Results

5.1 Mechanical Analysis

5.1.1 Native Lung Tissue

Native tissue samples were collected as previously described and tested at a rate of 1% strain/s. To examine the tissue's ability to resist deformation, known as the elastic modulus, the force and displacement data collected from the Instron was converted into stress (σ) and strain (ε), respectively, based on the sample dimensions

$$\sigma(t) = \frac{F(t)}{A} \quad (eq. 6)$$

$$\varepsilon(t) = \frac{\Delta L}{L} \quad (eq. 7)$$

Where for the stress equation, F is the force applied by the instrument at a given moment and A is the initial cross-sectional area of the specimen. The strain was calculated from the initial length, L, and the change in length from the initial length at a given moment, ΔL.

It was found that the stress-strain relationship is not linear between 10% and 20% strain. This is supported by the widely-recognized notion that strain-hardening occurs in lung parenchymal tissue [56]. Due to this, Hooke's Law relating stress and strain cannot be employed to determine the elastic (Young's)

modulus. In its place, the tangent modulus at a given strain was determined to provide a comparison between the native and engineered tissue.

An exponential fit was applied to the data to create the fit line. A small portion of the data, from 0% to 40%, was used to ensure an accurate fit over the region of interest. The tangent modulus was calculated from the fit line at three strain points; 10%, 15%, and 20%. These points were chosen based on the typical strain experienced by the human lung under normal breathing conditions.

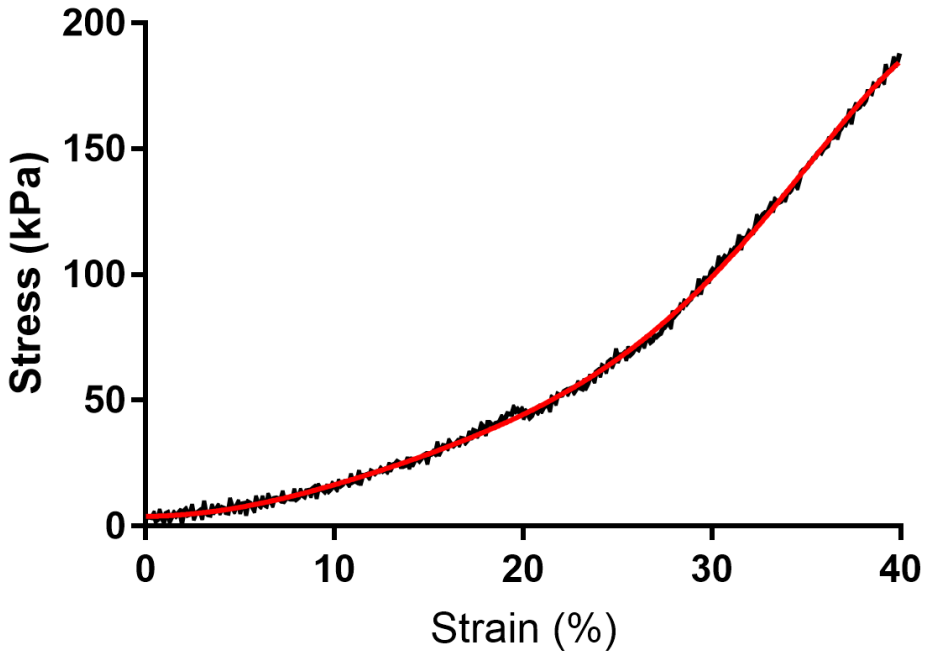

Figure 18:Representative calculated stress vs strain curve from experimental data (black) for a single lung tissue sample. An exponential fit line was applied to the data to determine the tangent modulus (R^2 = 0.9991).

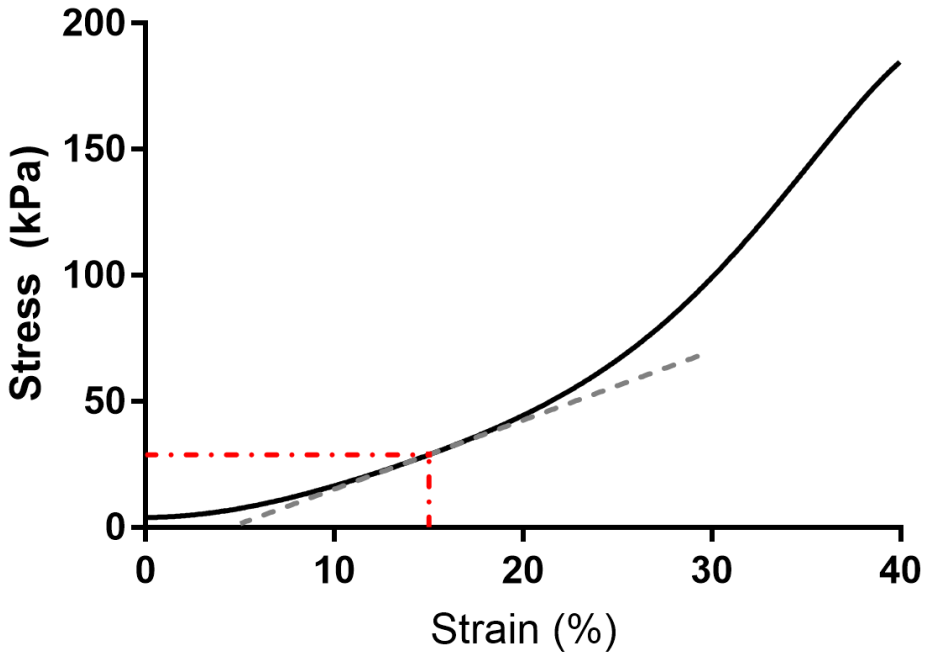

Figure 19: Representative sample showing tangent line at 15% strain calculated from the data fit line to determine the tangent modulus of the lung tissue at the given strain.

Table 2: Mean tangent modulus (± std dev.) for all lung tissue specimens calculated at strains of 10%, 15%, and 20%. A total of n=34 samples were collected from 4 lung specimens for testing. After outliers were removed, a total of n=31 samples were included.

Strain (%)	Tangent Modulus (kPa) All samples	Tangent Modulus (kPa) Outliers removed
10	155 (±222.4)	124 (±65.83)
15	205 (±241.3)	143.5 (±105.1)
20	271.4 (±250.5)	226.2 (±172.5)

5.1.2 Silk-Collagen Hydrogel

The engineered hydrogel tissue was analyzed using two methods; single load tensile test and a combination of cyclic load and single load tensile test. Initial single load failure analysis provided a baseline as well as provided insight into the behavior of the material over time. From this, it was found that the stiffness of this hydrogel increases over time. This is likely due to a couple factors. Over time, the fibroblast cells within the gel propagate, extending throughout the gel construct. Additionally, silk has been shown to self-align and crystalize over time. From this analysis, no significant difference was found between the hydrogel and the native lung tissue.

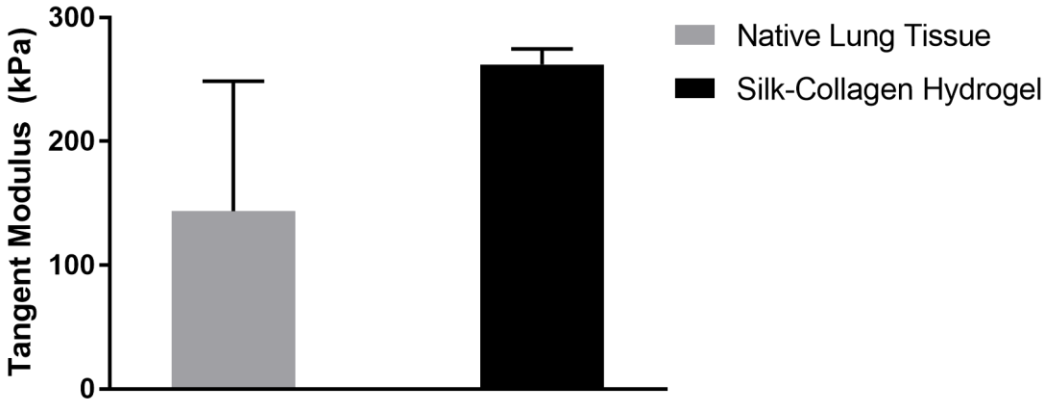

Figure 20: Comparison of the mean tangent modulus (+SD) of the native lung tissue specimens and the silk collagen hydrogel from single load tension test. Properties were considered statistically different if P<0.05 using one-way ANOVA and Tukey's multiple comparison tests.

Since the human lung is a continuously cyclic mechanism, it is important to understand how the hydrogel behaves under similar conditions. Two studies were conducted to examine how the mechanical properties of the engineered tissue behave after cyclic loading.

The initial cyclic load study examined the tangent modulus of the hydrogel using the same 1% strain/s strain rate the single load tensile test was conducted with. This provided a direct comparison between the single load and the cyclic load. The material was cyclically loaded 20 times before subjecting the samples to increasing force until failure occurred. The samples were tested at day 7 after plating.

For the second study, the hydrogel was subjected to 20 cycles at a rate of 9.33%strain/s. As mentioned, after completing the cyclic process, the sample was then subjected to increasing force until failure occurred.

In both cyclic studies, the tangent modulus of the hydrogel after being subjected to cyclic loading was found to be higher than those samples only loaded to failure. It is possible that with cyclic tension, the silk further aligns in crystalline structures. All hydrogel studies were performed with n=3 samples. No significant difference was found between the single load tension test and the cyclic load tests. When compared to the native lung tissue however, statistical significance was found between the two cyclic studies and the tissue.

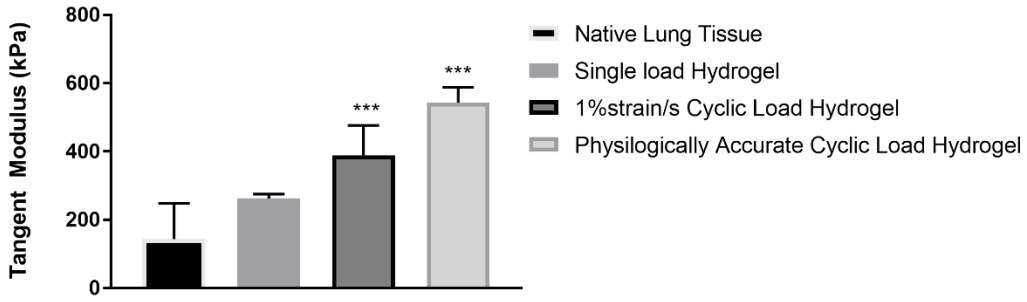

Figure 21: Comparison of the average tangent modulus at 10% strain (+SD) of the silk-collagen hydrogel due to single load tension test, cyclic loading at 1% strain/s, and cyclic loading at physiologically accurate conditions at day 7 after plating to the native lung tissue. Properties were considered statistically different if $P<0.05$ using one-way ANOVA and Tukey's multiple comparison tests.

Another important factor to consider when cyclic loading occurs is the effects of the phenomena of hysteresis. Hysteresis occurs when not all of the energy expended during expansion is recovered during relaxation as the result of the material not being purely elastic but rather viscoelastic. This is seen in Figure 22 with the crescent shape formed by loading (upper curve) and unloading (lower curve) curves. If the material was able to recover all expended energy, these curves would overlap one another without discrepancy. It is known that lung tissue is viscoelastic. Through this cyclic loading experiment, it was found that hysteresis is present in the hydrogel.

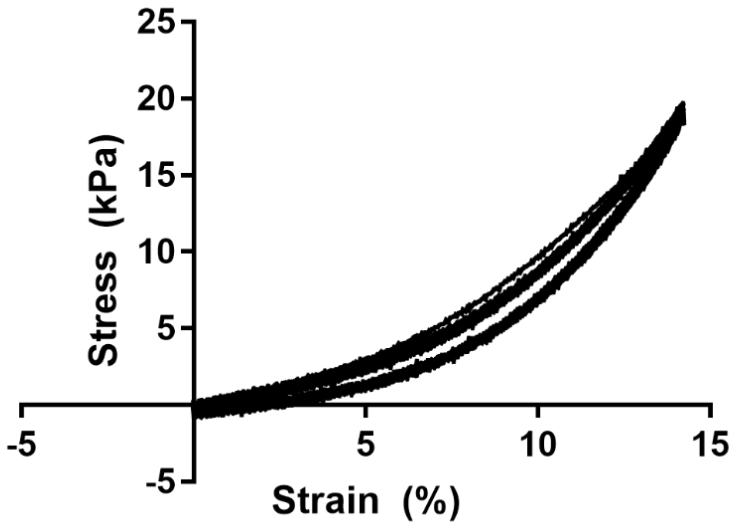

Figure 22: Representative stress- strain curve compilation. The loading/unloading curve for all 20 cycles within the test are shown. The discrepancy between the loading (upper curve) and unloading (lower curve) curves show that hysteresis is present within the material.

Hyaluronic Acid

Preliminary analysis of the addition of HA into the silk-collagen were also conducted. The addition of HA has been investigated because has been found to inhibit or reduce changes in the tangent modulus over time [66]. Unless affected by a disease such as Pulmonary Fibrosis, lung tissue does not significantly stiffen over time. Having the ability to fine tune the tangent modulus would allow for greater range of this system. Since this study was only preliminary, it was conducted using hydrogels not seeded with fibroblast cells.

Like the non-HA hydrogel, the tangent modulus was calculated from the stress-strain curve of a single-pull tension test. Cyclic load testing has not been conducted to date for this hydrogel composition. As seen in Figure 22, the tangent modulus does not have as great of variation between the two days of sample collection as seen with the hydrogel composition without HA when plated without cells.

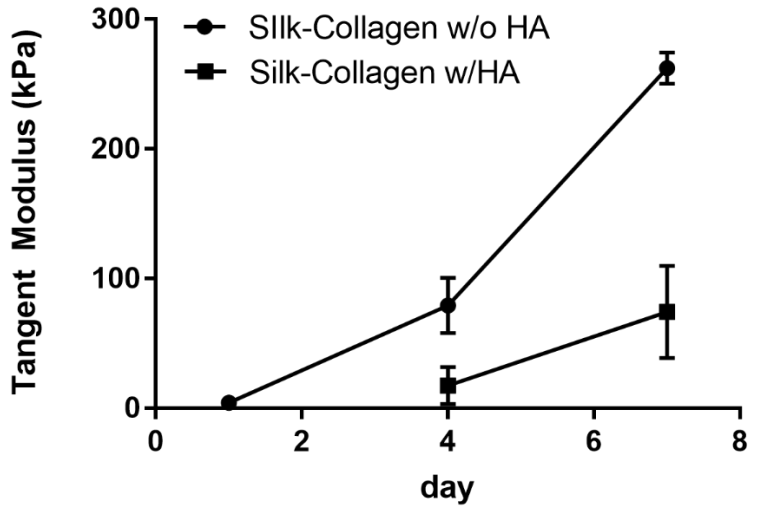

Figure 23: Comparison of the tangent modulus over time for the silk-collagen hydrogel with and without the addition of HA

The largest point of concern on for this composition is the potential for phase separation. Phase separation of the HA from the rest of the hydrogel matrix has been seen in previous studies conducted using only HA and not HRP. During the first batch of hydrogels constructed, heterogeneity appeared around day 7 and became well defined by day 10, as seen by the white regions highlighted in Figure 23. These regions are believed to be phase separation and not contamination as they appeared throughout the entirety of the hydrogel rather than just the surface. A follow up batch of hydrogel constructs were created for histological analysis and for which results will be discussed in 5.2. These hydrogels did not have the visible heterogeneous regions as seen in the initial batch. It is unclear on the reason for this however it is possible that the gel solution was not significantly mixed before pipetting onto the Tissue Train Plate for gelation.

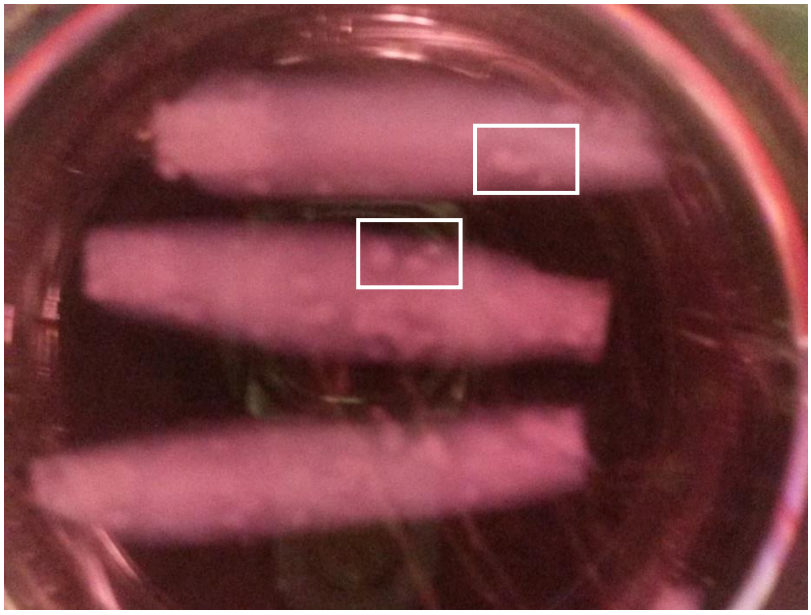

Figure 24: Silk-Collagen hydrogel strips with the addition of hyaluronic acid 10 days after plating. The regions bounded by white highlight regions of heterogeneity seen as white regions within the pink hydrogel.

5.2 Histology

5.2.1 Native Lung Tissue

During tissue sample collection for the mechanical analysis, samples were also collected for histological staining. These samples were collected from the same lobe of tissue that the mechanical analysis samples were collected from to provide qualitive insight into the tissue that was being studied.

In general, the regions void of the tissue shown in Figures 24 and 25 are likely alveolar regions. In Figure 25, the region within the box is morphologically different than the regions surrounding it. Unlike other regions in the image, there are thick walls surrounding the two main voids. Beyond morphology, the largely pink coloring suggests that this region has high concentrations of collagen. The combination of these differences suggest that this region is showing cross-sections of bronchioles.

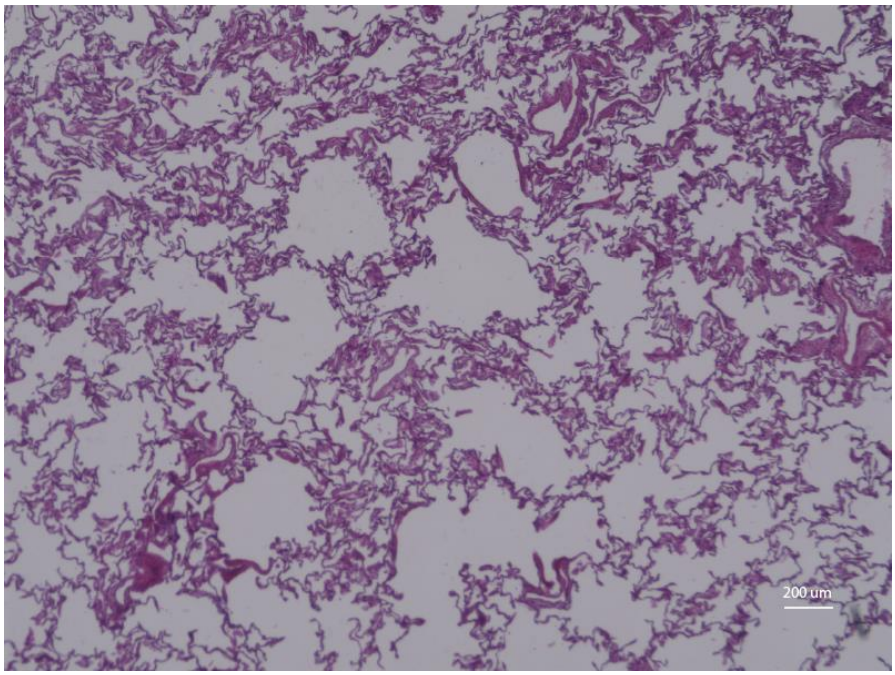

Figure 25: H&E-stained lung tissue section imaged at 10x magnification. Scale shown is 200µm.

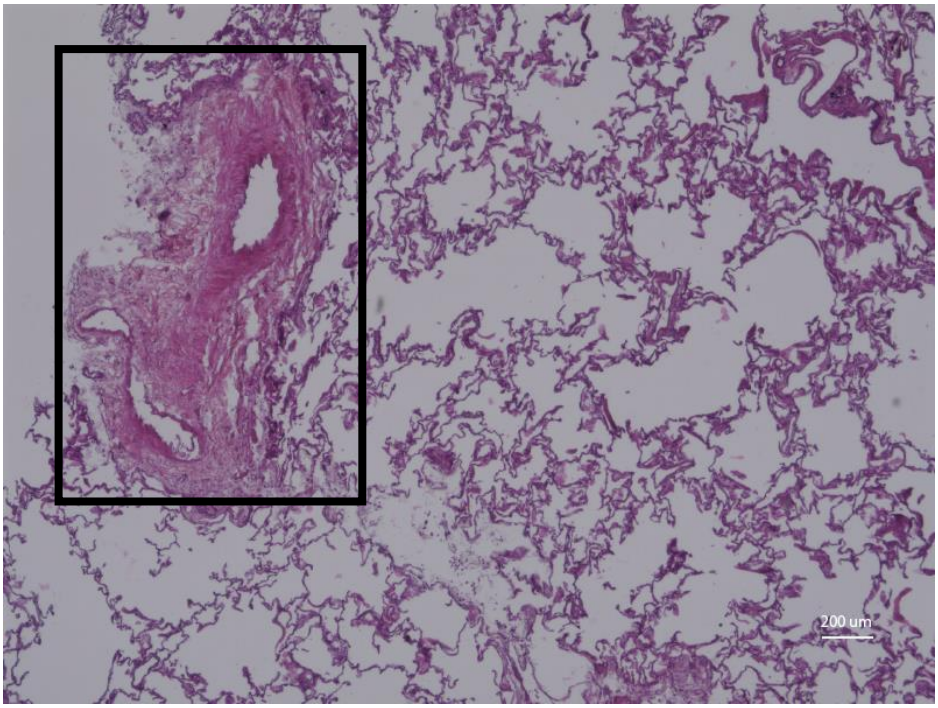

Figure 26: H&E-stained lung tissue section. The region within the black box is likely a bronchiole cross section. Scale shown is 200µm.

5.2.2 HA Hydrogel

As previously discussed, the phase separation seen by eye in the first round of hydrogel plating was not visible during the second plating. Regardless, samples were collected at days 1,4,7, and 10 for histological analysis. Serial sections from each time point were separated into two groups to be stained with either H&E Alcian Blue. Over time, the microscopic heterogeneity within the hydrogel becomes visible as seen in both staining methods. The heterogeneity appears consistent across the two staining methods, suggesting that is progression is the crosslinking and crystalline alignment of the silk and collagen with the HA.

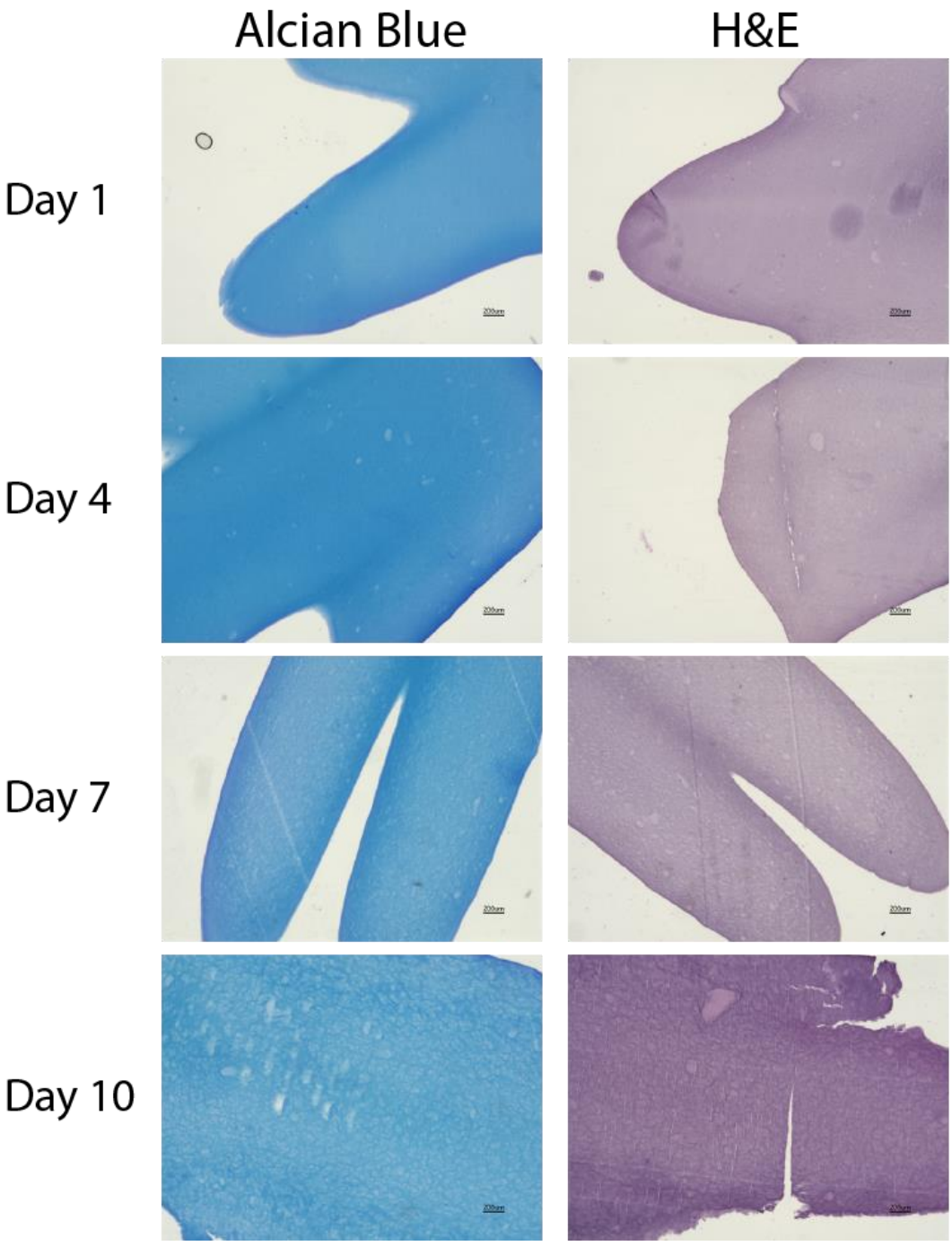

Figure 27: Histological time lapse of the silk-collagen hydrogel with the addition of HA. Samples on the left were stained with Alcian Blue to indicate the presence of HA. Samples on the right were stained with H&E to indicate the presence of collagen. Over time, both staining methods show heterogeneity within the gel. Scale shown is 200 μm.

5.3 Bioreactor

5.3.1 Alveolus

The alveolus model was initially cast out of PDMS to develop the method before moving on to fabricating it out of the hydrogel. While not an exact substitute, developing the method for fabrication with PDMS first allowed for fine tuning of a process before moving onto the hydrogel. As previously mentioned, the PDMS model formation was conducted as close to conditions that would be needed for sterile construction and assembly. This included limiting/eliminating contact with the PDMS model while removing it from the mold.

As discussed in 3.1, handling of the hydrogel during transport was conducted using only sterile tweezers and spatula to prevent contamination.

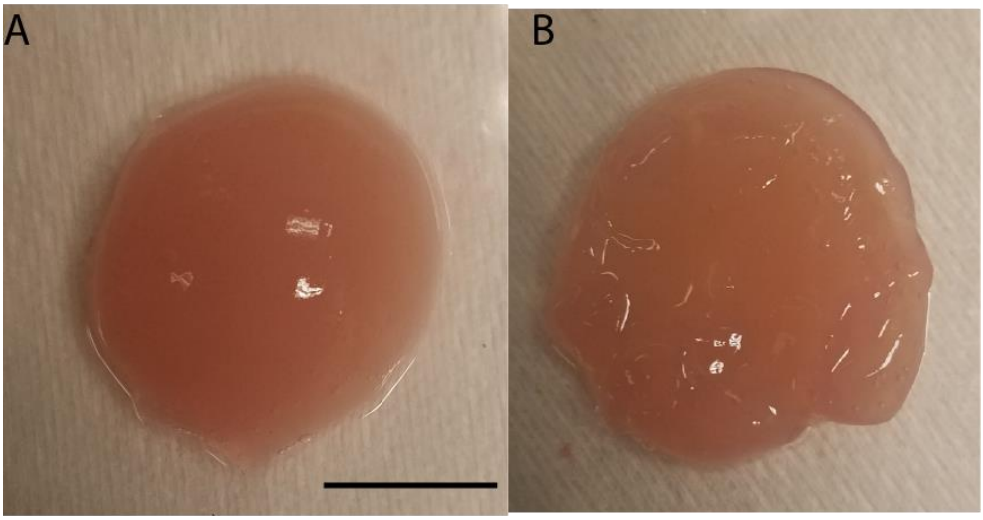

Figure 28: Cross section of the hydrogel alveolus shown from (A) the outer surface and (B) the inner surface. The bronchiole neck was removed during dissection. Scale shown is 10mm

5.3.2 Chamber

With minor modification, the chamber was found to be sufficiently liquid and air tight. While there was no liquid leak, during removal of media, air bubbles were initially seen around the grommet/tube inlets at the bottom of the chamber, a sign of air leakage. To remedy this, UV curable adhesive was used to seal around the grommets and tubing on the outer edge of the chamber.

4.3.3 System

From the average inner volume of the alveolus model, the parameters for the Syringe Pump device were calculated as discussed in 4.5.3 These values are summarized in Table 3. The pressure difference was calculated from Boyle's Law shown in Equation 1.

The media infusion/withdraw rate was calculated as discussed in 4.5.3. It was calculated to be 10.05 mL/min for 1.88 seconds per step in the cycle. To fully program the Syringe Pump, this flow rate was input along with the change total volume to be extracted/infused. Inputting these values directly into the pump interface to create the continuous cycle was a straightforward process for the basic cycle being used. Using the associated computer program increased ease of use and ability to make modifications. The volumes and pressures within the system components during the cycle are summarized in Tables 3-5.

Table 3: Summary of the volume (V) and pressure (P) initial conditions for the alveolus cavity and the syringe, assuming 10 mL of media is preloaded in the syringes.

	V (mL)	P (kPa)
Alveolus	1.436	101.3
Syringe/Chamber	35.38	101.3

Table 4: Summary of the volume and pressure changes of the alveolus cavity and syringe during inspiration. assuming a total of 10 mL is preloaded in the syringes. At the beginning, the syringe withdraws, decreasing the pressure within the chamber/syringe subsystem. During the middle stage, the alveolus expands to match the pressure decrease, resulting in a pressure differential with the atmosphere. At the end, air is drawn into the alveolus to balance the pressure differential, creating a new differential between the chamber/syringe subsystem and the alveolus.

	Beginning		Middle		End	
	V (mL)	P (kPa)	V (mL)	P (kPa)	V (mL)	P (kPa)
Alveolus	1.436	101.3	3.618	95.42	3.618	101.42
Syringe/Chamber	37.57	95.42	37.57	95.42	37.57	95.42

Table 5: Summary of the volume and pressure changes of the alveolus cavity and syringe during expiration. assuming a total of 10 mL is preloaded in the syringes. At the beginning, the syringe retracts, increasing the pressure within the chamber/syringe subsystem. During the middle stage, the alveolus contracts to match the pressure decrease, resulting in a pressure differential with the atmosphere. At the end, air is removed from the alveolus to balance the pressure differential, creating a new differential between the chamber/syringe subsystem and the alveolus.

	Beginning		Middle		End	
	V (mL)	P (kPa)	V (mL)	P (kPa)	V (mL)	P (kPa)
Alveolus	3.618	101.3	1.436	108.0	1.436	101.3
Chamber/Syringe	33.20	108.0	33.20	108.0	33.20	108.0

Chapter 6: Discussion and Future Work

6.1 Material Analysis

6.1.1 Discussion

The large deviation within the lung tissue dataset, when compared to that of the hydrogel, can be explained in part to natural variation in the donor tissue. A total of four donors were sampled. Donor acceptance protocol was in place to alleviate some variables that could account for donor to donor variation however no two donors' history and biological makeup are the same. Another factor that could account for variation is the presence of the pleura on the sample. While not intended, variation may have arisen if some samples tested had the pleura while others did not.

From the results of the comparison between the three hydrogel studies, it was found that the hydrogel experiences strain hardening/ stiffening. These results are consistent with results from previous studies on protein based hydrogels [56]. This is also consistent with results from the native tissue study and related published findings for soft biological tissue [26]. It is also possible that this is a temporary phenomenon and that the strain hardening only initially occurs and then strain softening occurs. Further work would need to be conducted using a larger number of cycles during cyclic loading to determine this. Statistical analysis using one-way ANOVA and Tukey's multiple comparison show no statistical significance difference amongst the three hydrogel tension tests

performed ($P > 0.05$). Statistical significance ($P < 0.05$) was found however through comparison between the native lung tissue and the two cyclic loading tests. Despite the statistical significance between the native lung tissue and the engineered tissue, increased stiffness may be suitable for modeling diseases such as pulmonary fibrosis which exhibit stiffening as compared to healthy tissue.

The difference between the stress during loading and during unloading during the cyclic tests concludes that the hydrogel, like lung tissue, is not perfectly elastic. This is consistent with the behavior of lung tissue This curve is similar to results seen in cyclic loading studies of native lung tissue [24,49].

6.1.2 Future Work

The cyclic load studies completed used a relatively low number of cycles, relating to only ~1.5 minutes of breathing. Further studies examining extended cyclic loading (e.g. 2 hours) will help to further define the mechanical behavior of the engineered tissue. Once a fully operational system is developed, the tangent modulus of the hydrogel after completing a determined number of cycles within the system should be evaluated. This would be performed using the same parameters as the initial single load tension test discussed in 5.1.2.

To further quantify similarities between engineered and native tissues, a gas diffusion study should also be completed. As discussed in 2.2, the major result of many lung diseases is the limitation of gas exchange across the alveolar wall.

This quantification will allow for future integration of the respiration process into the system.

Further studies analyzing the properties of the hydrogel with the inclusion of HA should be conducted to determine if it is a viable option as an engineered tissue model for human lung tissue. This material shows promise for extending the longevity of studies as well as the number of diseases that can be studied with this model. Since the elasticity of the material has been shown to remain relatively constant over time, diseases that do not cause stiffening over time will not have to be studied during the time frame that the gel is within the desired elasticity.

6.2 System Function

6.2.1 Discussion

To date, the assembly method has been successfully employed to create a working PDMS model however has not successfully created a working hydrogel model. The challenge limiting success stems from creating an air tight seal between the segment of tubing and the alveolus construct. The hydrogel constructs need to be handled with great care to prevent rips in the material. Additionally, the stress concentration of the clamp or zip tie around the hydrogel and tubing lead to weak points in the material. This problem may be alleviated through use of a fully hydrogel model, such as one of the initial designs considered. This will come with its own set of challenges however it should eliminate the need to clamp the hydrogel to another material.

Another option to explore to alleviate this problem would be to encase a PDMS with the hydrogel. This would provide the robustness of the PDMS with the desired properties for cell growth and proliferation of the hydrogel. There is the potential that this would limit the variety of cells which could be incorporated and it may result in a change in mechanical behavior of the hydrogel over time however to know for sure multiple studies would need to be conducted.

Beyond using a set of molds to create the hydrogel alveolus, alternative methods such as 3D bioprinting could be investigated. For this method to be successful, alterations to the hydrogel preparation protocol would need to be made to account for the higher viscosity needed to print objects with a 3D printer. Cell viability after printing would also need to be examined.

6.2.2 Future Work

As mentioned, continuing work needs to be conducted to produce a hydrogel model that will "breathe" within the chamber. This could include developing a new suspension method for the alveolus or continuing with one of the methods explored though this work.

As with initial material analysis, lung fibroblast cells should be integrated into the alveolus model. This would be completed by using the method described in 4.3.1 for 3D cell culture. A viability study should be conducted to ensure that the fibroblasts remain healthy over a determined period of time. After successful integration of fibroblasts into the engineered alveolus, protocol to integrate endothelial and epithelial cells should be developed. Integration of the epithelial

cells will allow researchers to study the surfactant layer and related surface tension discussed in 2.2.

There is the potential for some discrepancy between the theoretical values calculated for the volume and pressure change calculated to achieve the maximum strain and the actual values. This discrepancy would be caused factors such as air entering/leaving the system at undesired locations such as well as radial variations from the average value. Additionally, the model was simplified as a perfect sphere and effects of surface tension were neglected. To measure the actual pressure differential throughout the duration of the system function, a pressure sensor can be attached to both the inside of the alveolus as well as the within the chamber. A strain gauge would allow for measurement of the strain throughout the study as well.

Chapter 7: Conclusion

The designed bioreactor was partially successful at achieving the objectives defined within the scope of the project. A fully sealed chamber capable of being sterilized was constructed to contain an engineered tissue model of a lung tissue alveolus. The Syringe Pump system can be easily fine-tuned to the desired specifications and to cycle for one or many cycles. The system was successfully employed to cyclically deform both a balloon and PDMS model however there is still room for improvement to enable the engineered tissue model to follow suit. Limitations to the model come largely from the fragility of the gel while handling to construct the system.

Material analysis of the silk-collagen hydrogel and of human lung tissue samples showed significant difference after cyclic loading of the hydrogel. Further analysis should be conducted to confirm this through high cycle analysis before changing the hydrogel composition as there is the potential that the material initially exhibits cycle hardening which will subsides during long term cycles. This material may also be well suited for modeling diseased tissue, as increased stiffness is a major component of the effect of lung diseases on the tissue. The addition of HA into the silk-collagen hydrogel has shown promise to further tune the hydrogel to fit the mechanical properties of the hydrogel. Further analysis of the silk-collagen hydrogel with the inclusion of HA should be conducted to confirm this and ensure that phase separation will not occur.

Overall, with slight modifications and further analysis, this model shows promise to make the next step forward in cell culture tissue models to replace animal models or clinical studies.

References

[1] *About PF*. 2017; Available from: http://www.pulmonaryfibrosis.org/life-with-pf/about-pf.

[2] *American Lung Association*. 2017; Available from: http://www.lung.org/.

[3] *Anatomy and physiology of the lung - Canadian Cancer Society*. 2017; Available from: http://www.cancer.ca/en/cancer-information/cancer-type/lung/lung-cancer/the-lungs/?region=on.

[4] Zhao, S., et al., *Bio-functionalized silk hydrogel microfluidic systems.* Biomaterials, 2016. **93**: p. 60-70.

[5] Caló, E. and V.V. Khutoryanskiy, *Biomedical applications of hydrogels: A review of patents and commercial products.* European Polymer Journal, 2015. **65**: p. 252-267.

[6] Kluge, J.A., et al., *Bioreactor System Using Noninvasive Imaging and Mechanical Stretch for Biomaterial Screening.* Annals of Biomedical Engineering, 2011. **39**(5): p. 1390-1402.

[7] Tanaka, R. and M.S. Ludwig, *Changes in viscoelastic properties of rat lung parenchymal strips with maturation.* Journal of Applied Physiology, 1999. **87**(6): p. 2081.

[8] Cheng, W., et al., *Contribution of opening and closing of lung units to lung hysteresis.* Respiration Physiology, 1995. **102**(2): p. 205-215.

[9] O'Neill, J.D., et al., *Decellularization of Human and Porcine Lung Tissues for Pulmonary Tissue Engineering.* The Annals of Thoracic Surgery. **96**(3): p. 1046-1056.

[10] Nichols, J.E., J.A. Niles, and J. Cortiella, *Design and development of tissue engineered lung: Progress and challenges.* Organogenesis, 2009. **5**(2): p. 57-61.

[11] Price, A.P., et al., *Development of a Decellularized Lung Bioreactor System for Bioengineering the Lung: The Matrix Reloaded.* Tissue Engineering. Part A, 2010. **16**(8): p. 2581-2591.

[12] Gardel, M.L., et al., *Elastic Behavior of Cross-Linked and Bundled Actin Networks.* Science, 2004. **304**(5675): p. 1301.

[13] Nichols, J.E. and J. Cortiella, *Engineering of a complex organ: progress toward development of a tissue-engineered lung.* Proc Am Thorac Soc, 2008. **5**(6): p. 723-30.

[14] Suki, B. and J.H.T. Bates, *Extracellular matrix mechanics in lung parenchymal diseases.* Respiratory physiology & neurobiology, 2008. **163**(1-3): p. 33-43.

[15] Golden, A.P. and J. Tien, *Fabrication of microfluidic hydrogels using molded gelatin as a sacrificial element.* Lab Chip, 2007. **7**(6): p. 720-5.

[16] *General Information about Pulmonary Fibrosis*. 2017; Available from: https://www.thoracic.org/patients/lung-disease-week/2015/pulmonary-fibrosis-week/general-info.php.

[17] Partlow, B.P., et al., *Highly tunable elastomeric silk biomaterials.* Advanced functional materials, 2014. **24**(29): p. 4615-4624.

[18] Huh, D., et al., *A Human Disease Model of Drug Toxicity–Induced Pulmonary Edema in a Lung-on-a-Chip Microdevice.* Science Translational Medicine, 2012. **4**(159): p. 159ra147-159ra147.
[19] Ellis, R. *Hyaluronidase Alcian Blue Staining Protocol*. 2017; Available from: http://www.ihcworld.com/_protocols/special_stains/hyaluronidase_alcian_blue_ellis.htm.
[20] Tibbitt, M.W. and K.S. Anseth, *Hydrogels as Extracellular Matrix Mimics for 3D Cell Culture.* Biotechnology and bioengineering, 2009. **103**(4): p. 655-663.
[21] Liu, J., et al., *Hydrogels for Engineering of Perfusable Vascular Networks.* International Journal of Molecular Sciences, 2015. **16**(7): p. 15997-16016.
[22] Peppas, N.A., et al., *Hydrogels in Biology and Medicine: From Molecular Principles to Bionanotechnology.* Advanced Materials, 2006. **18**(11): p. 1345-1360.
[23] Choe, M.M., P.H.S. Sporn, and M.A. Swartz, *An in vitro airway wall model of remodeling.* American Journal of Physiology - Lung Cellular and Molecular Physiology, 2003. **285**(2): p. L427.
[24] Brewer, K.K., et al., *Lung and alveolar wall elastic and hysteretic behavior in rats: effects of in vivo elastase treatment.* Journal of Applied Physiology, 2003. **95**(5): p. 1926.
[25] White, E.S., *Lung Extracellular Matrix and Fibroblast Function.* Annals of the American Thoracic Society, 2015. **12**(Suppl 1): p. S30-S33.
[26] Suki, B., D. Stamenovic, and R. Hubmayr, *Lung Parenchymal Mechanics.* Comprehensive Physiology, 2011. **1**(3): p. 1317-1351.
[27] Suki, B. and J.H.T. Bates, *Lung tissue mechanics as an emergent phenomenon.* Journal of Applied Physiology, 2011. **110**(4): p. 1111-1118.
[28] Konar, D., et al., *Lung-On-A-Chip Technologies for Disease Modeling and Drug Development.* Biomedical Engineering and Computational Biology, 2016. **7**(Suppl 1): p. 17-27.
[29] Rockwood, D.N., et al., *Materials fabrication from Bombyx mori silk fibroin.* Nat. Protocols, 2011. **6**(10): p. 1612-1631.
[30] Zeng, Y.J., D. Yager, and Y.C. Fung, *Measurement of the Mechanical Properties of the Human Lung Tissue.* Journal of Biomechanical Engineering, 1987. **109**(2): p. 169-174.
[31] Mitzner, W., *MECHANICS OF THE LUNG IN THE 20(TH) CENTURY.* Comprehensive Physiology, 2011. **1**(4): p. 2009-2027.
[32] Khademhosseini, A. and R. Langer, *Microengineered hydrogels for tissue engineering.* Biomaterials, 2007. **28**(34): p. 5087-5092.
[33] Mandal, B.B., et al., *Multilayered silk scaffolds for meniscus tissue engineering.* Biomaterials, 2011. **32**(2): p. 639-651.
[34] Gomes, S., et al., *Natural and genetically engineered proteins for tissue engineering.* Progress in Polymer Science, 2012. **37**(1): p. 1-17.

[35] Nickerson, C.A. and C.M. Ott, *A New Dimension in Modeling Infectious Disease.*
[36] Storm, C., et al., *Nonlinear elasticity in biological gels.* Nature, 2005. **435**(7039): p. 191-194.
[37] Nichols, J.E., et al., *Novel in vitro respiratory models to study lung development, physiology, pathology and toxicology.* Stem Cell Research & Therapy, 2013. **4**(Suppl 1): p. S7-S7.
[38] Ochs, M., et al., *The number of alveoli in the human lung.* Am J Respir Crit Care Med, 2004. **169**(1): p. 120-4.
[39] Andrikakou, P., K. Vickraman, and H. Arora, *On the behaviour of lung tissue under tension and compression.* Sci Rep, 2016. **6**: p. 36642.
[40] Skardal, A., T. Shupe, and A. Atala, *Organoid-on-a-chip and body-on-a-chip systems for drug screening and disease modeling.* Drug Discovery Today, 2016. **21**(9): p. 1399-1411.
[41] *Plastics Compatability with Sterilization Methods*. 2017; Available from: https://www.industrialspec.com/resources/plastics-sterilization-compatibility.
[42] Charalampidis, C., et al., *Pleura space anatomy.* Journal of Thoracic Disease, 2015. **7**(Suppl 1): p. S27-S32.
[43] Lamba, N.M.K., K.A. Woodhouse, and S.L. Cooper, *Polyurethanes in Biomedical Applications*. 1997: Taylor & Francis.
[44] Floren, M., C. Migliaresi, and A. Motta, *Processing Techniques and Applications of Silk Hydrogels in Bioengineering.* J Funct Biomater, 2016. **7**(3).
[45] Staff, M.C. *Pulmonary edema Treatments and drugs*. 2017; Available from: http://www.mayoclinic.org/diseases-conditions/pulmonary-edema/basics/treatment/con-20022485.
[46] Ikegami, M., et al., *Pulmonary Surfactant Surface Tension Influences Alveolar Capillary Shape and Oxygenation.* American Journal of Respiratory Cell and Molecular Biology, 2009. **41**(4): p. 433-439.
[47] Huh, D., et al., *Reconstituting Organ-Level Lung Functions on a Chip.* Science, 2010. **328**(5986): p. 1662.
[48] Sugihara, H., et al., *Reconstruction of alveolus-like structure from alveolar type II epithelial cells in three-dimensional collagen gel matrix culture.* The American Journal of Pathology, 1993. **142**(3): p. 783-792.
[49] Demory, D., et al., *Recruitability of the lung estimated by the pressure volume curve hysteresis in ARDS patients.* Intensive Care Med, 2008. **34**(11): p. 2019-25.
[50] Kumar Mahto, S., et al., *Respiratory Physiology on a Chip.* Scientifica, 2012. **2012**: p. 12.
[51] Khetan, S., J.S. Katz, and J.A. Burdick, *Sequential crosslinking to control cellular spreading in 3-dimensional hydrogels.* Royal Society of Chemistry, 2009. **5**(8): p. 1601-1606.
[52] Vepari, C. and D.L. Kaplan, *Silk as a Biomaterial.* Progress in polymer science, 2007. **32**(8-9): p. 991-1007.

[53] Altman, G.H., et al., *Silk-based biomaterials.* Biomaterials, 2003. **24**(3): p. 401-416.
[54] Schmoller, K.M. and A.R. Bausch, *Similar nonlinear mechanical responses in hard and soft materials.* Nat Mater, 2013. **12**(4): p. 278-281.
[55] Cai, H., G. Azangwe, and D.E.T. Shepherd, *Skin cell culture on an ear-shaped scaffold created by fused deposition modelling.* Bio-Medical Materials and Engineering, 2005. **15**: p. 375-380.
[56] Cui, Y., et al., *Strain hardening and highly resilient hydrogels crosslinked by chain-extended reactive pseudo-polyrotaxane.* RSC Advances, 2014. **4**(100): p. 56791-56797.
[57] Kim, U.-J., et al., *Structure and Properties of Silk Hydrogels.* Biomacromolecules, 2004. **5**(3): p. 786-792.
[58] Staff, M.C. *Symptoms and causes - Mayo Clinic*. 2017; Available from: http://www.mayoclinic.org/diseases-conditions/pulmonary-fibrosis/symptoms-causes/dxc-20211754.
[59] Kim, U.-J., et al., *Three-dimensional aqueous-derived biomaterial scaffolds from silk fibroin.* Biomaterials, 2005. **26**(15): p. 2775-2785.
[60] Petersen, T.H., et al., *Tissue-engineered lungs for in vivo implantation.* Science, 2010. **329**(5991): p. 538-41.
[61] Sugihara, T., J. Hildebrandt, and C.J. Martin, *Viscoelastic properties of alveolar wall.* Journal of Applied Physiology, 1972. **33**(1): p. 93-98.
[62] *What Is COPD?* 2017; Available from: https://www.ncbi.nlm.nih.gov/pubmed/.
[63] Bates, J.H.T., Lung Mechanics: An Inverse Modeling Approach. 2009, United States of America: Cambridge University Press.
[64] Lamba, N.M.K., K.A. Woodhouse, and S.L. Cooper, Polyurethanes in Biomedical Applications. 1997: Taylor & Francis.
[65] Brown, D., *Thick-Walled Spherical Vessel*. 2017; Available from: http://www.vermontveterinarycardiology.com/index.php/for-cardiologists/for-cardiologists?id=206.
[66] Raia, N.R., et al., *Enzymatically crosslinked silk-hyaluronic acid hydrogels.* Biomaterials, 2017. **131:** p. 58-67